10
Techniques for exciting surface plasmons

Figures

10.1 Introduction

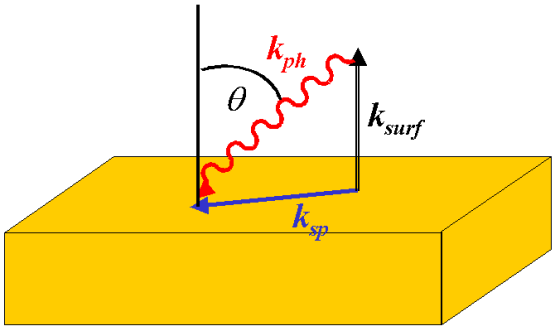

Fig. 10.1. Illustration of momentum conservation for optical excitation of a SP. The component of the wavevector of the incident photon, k_{ph}, which lies in the plane of the surface must equal the wavevector of the SP, k_{SP}.

10.2 Otto configuration

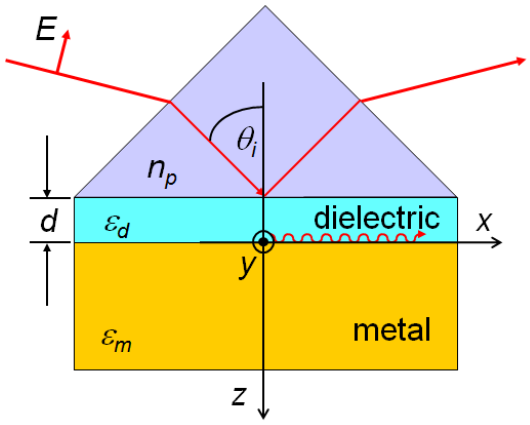

Fig. 10.2. Illustration of the Otto configuration for launching SPs. For later convenience, the coordinate system has been defined so that the origin occurs at the metal-dielectric interface and the positive *z*-direction is into the metal.

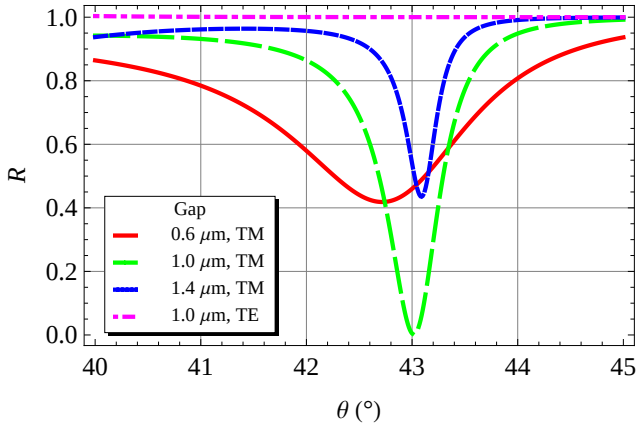

Fig. 10.3. Reflectivity as a function of angle of incidence, θ, for three different air gap spacings between a glass prism and a gold surface, for both TE and TM incident light. (*Mathematica* simulation.)

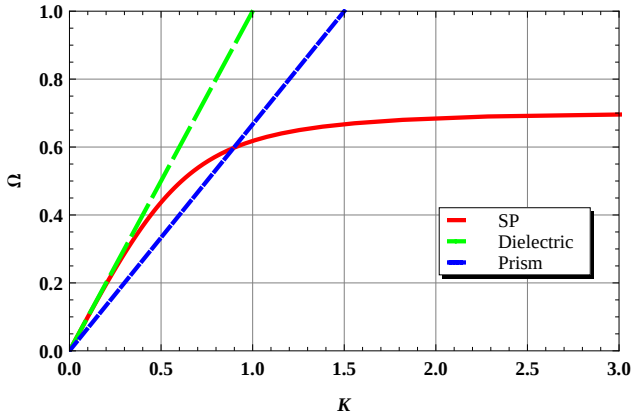

Fig. 10.4. Diagram illustrating wavector matching in the Otto configuration. The solid line is the SP dispersion curve. The long dashed line is the light line, or frequency/wavevector relation for light propagating in vacuum. The short dashed line is the light line within the high index prism. The point of intersection between the prism light line and the SP dispersion curve determines the SP excitation that satisfies energy and momentum conservation. (*Mathematica* simulation.)

10.3 Kretschmann configuration

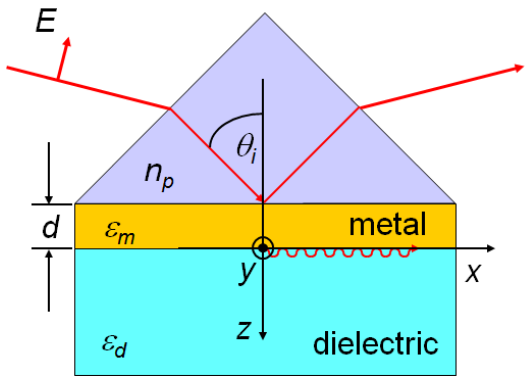

Fig. 10.5. Illustration of the Kretschmann configuration for launching SPs. For later convenience, the coordinate system has been defined so that the origin occurs at the metal-dielectric interface and the positive *z*-direction is into the metal.

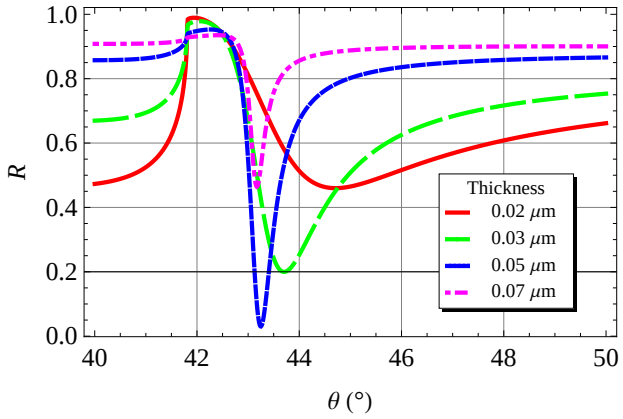

Fig. 10.6. Reflectivity of TM polarization at a wavelength of 800 nm as a function of angle of incidence, θ, for various thicknesses of gold films in the Kretschmann configuration with a glass prism and air below the gold. (*Mathematica* simulation.)

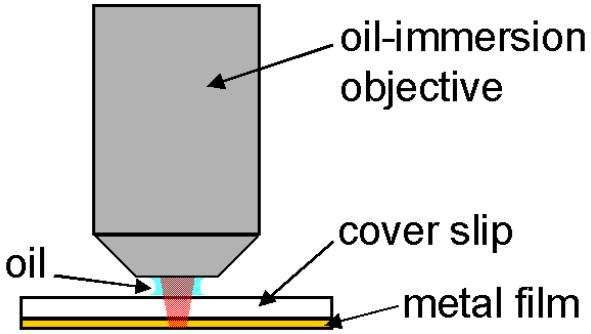

Fig. 10.7. Kretschmann configuration using an oil immersion objective.

10.4 Diffraction gratings and Wood's anomalies

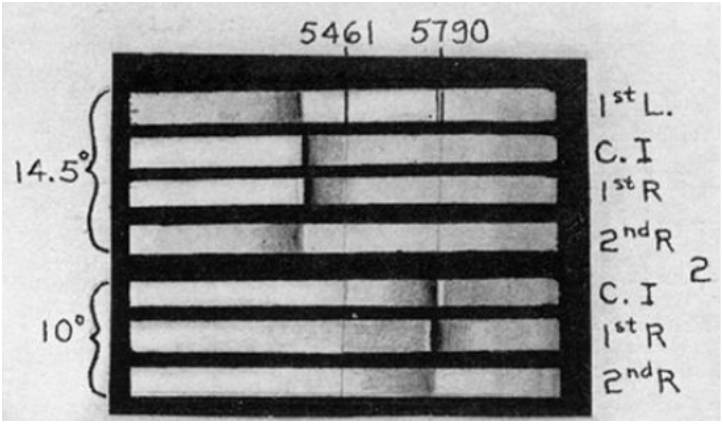

Fig. 10.8. An example of Wood's anomalies seen in the reflection spectra of diffraction gratings measured by R. W. Wood. Reprinted with permission from R. W. Wood, *Phys. Rev.* **48** 928 (1935). © 1935 by the American Physical Society. [6]

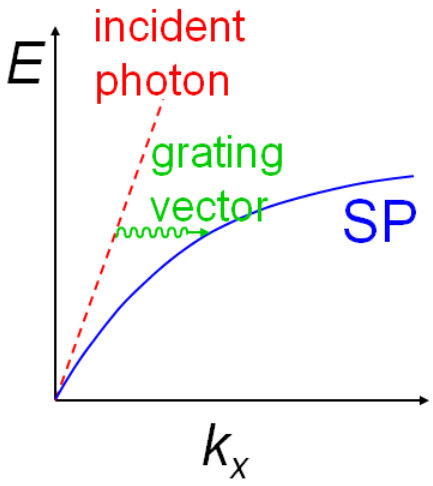

Fig. 10.9. The grating vector (wavy line) can supply the necessary momentum to an incident photon (dashed line) so that both energy and momentum may be conserved when exciting a surface plasmon (solid line). k_x is the component of the wavevector in the plane of the grating.

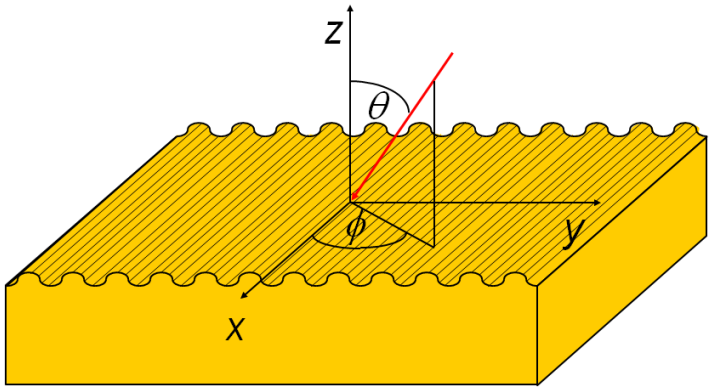

Fig. 10.10. A plane wave is incident onto a diffraction grating at a polar angle θ and an azimuthal angle ϕ with respect to the coordinate system as shown. The grooves are parallel to the *x*-direction.

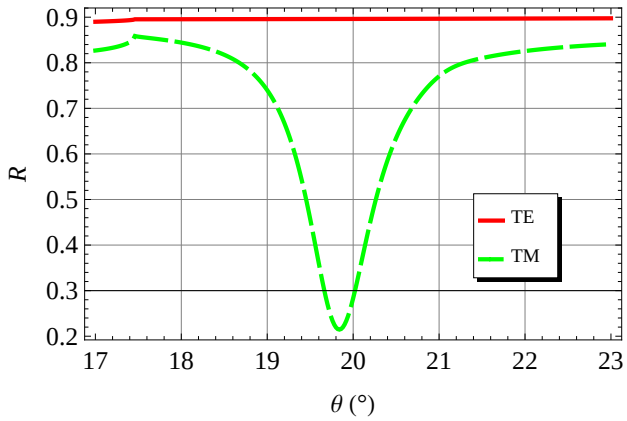

Fig. 10.11. Zero order reflectivity as a function of angle of incidence, θ, for a gold grating at a wavelength of 700 nm as described in the text. The plane of incidence is perpendicular to the grooves. The surface plasmon resonance in TM polarization occurs at θ~19.8°. (*Mathematica* simulation.)

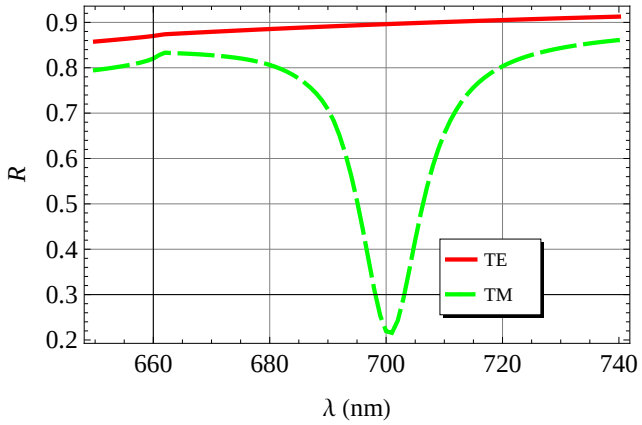

Fig. 10.12. Wood's anomaly in the reflectivity spectrum of a gold diffraction grating with incident beam at 19.5° and the plane of incidence perpendicular to the grooves. (*Mathematica* simulation.)

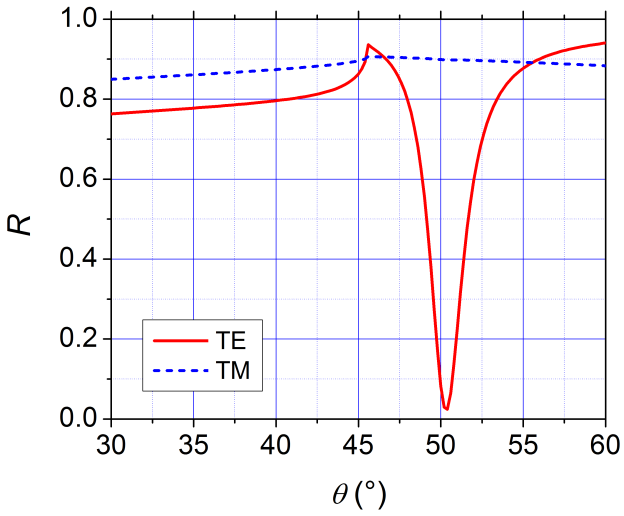

Fig. 10.13. Zero order reflectivity as a function of angle of incidence, θ, for a gold grating with a 1 μm period and 70 nm groove depth at a wavelength of 700 nm. The plane of incidence is parallel to the grooves.

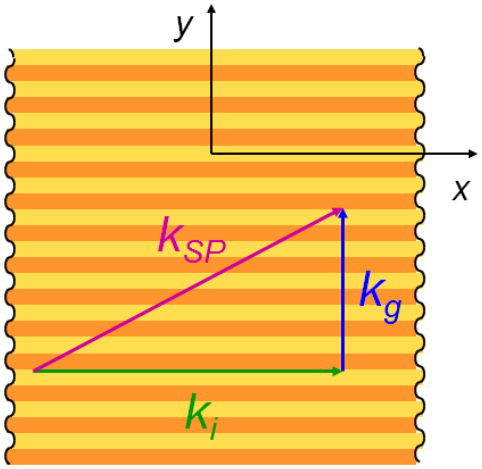

Fig. 10.14. When the plane of incidence is parallel to the grooves, the component of the incident wavevector in the plane of the grating, k_i, is perpendicular to the grating vector, k_g. The SP then propagates with wavevector k_{SP} at an angle to the grooves.

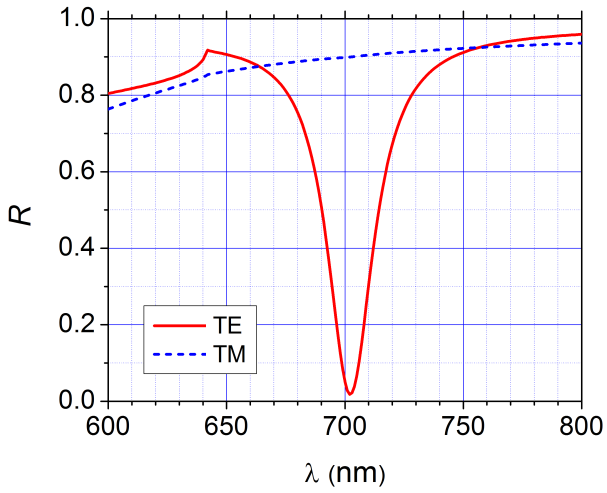

Fig. 10.15. Wood's anomaly in the reflectivity spectrum of a gold diffraction grating with incident beam at 50.0° and the plane of incidence parallel to the grooves. The wavelength dependence of the refractive index of gold is taken from the Drude-Lorentz fit. [8]

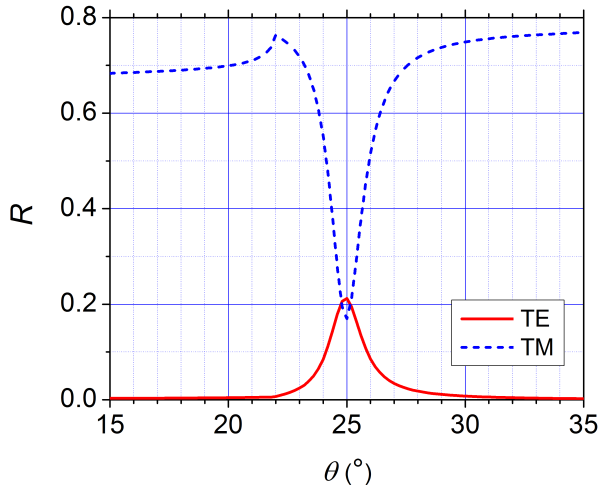

Fig. 10.16. Reflectivity as a function of angle of incidence, θ, for a gold grating with a 1 μm period and a groove depth of 90 nm at a wavelength of 700 nm. The plane of incidence is at an azimuthal angle of 45° to the grooves. The incident beam is TM polarized.

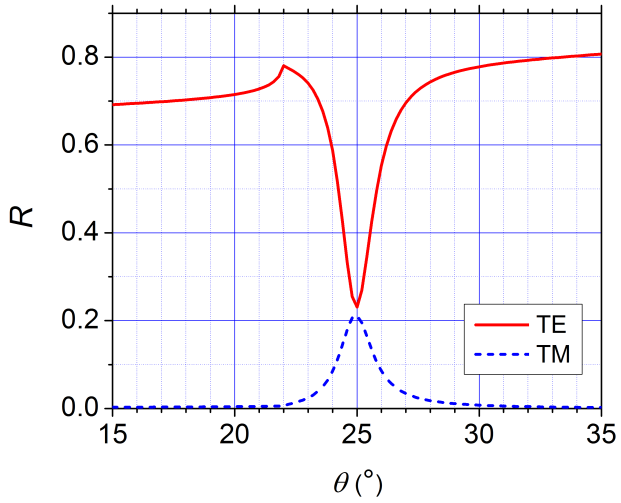

Fig. 10.17. Reflectivity as a function of angle of incidence, θ, for a gold grating with a 1 μm period and a groove depth of 90 nm at a wavelength of 700 nm. The plane of incidence is at an azimuthal angle of 45° to the grooves. The incident beam is TE polarized.

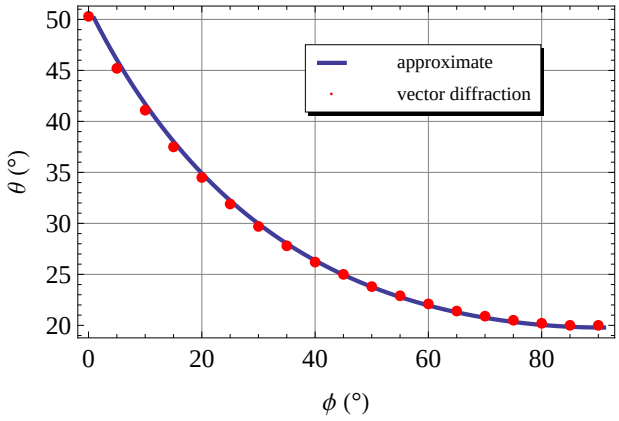

Fig. 10.18. Polar angle, θ, of the SP resonance for a gold grating with a 1 μm period at a wavelength of 700 nm as a function of azimuthal angle, ϕ. The results from rigorous vector diffraction theory (circles) are compared to the approximate relation of Eq. (10.7) (solid line). (*Mathematica* simulation.)

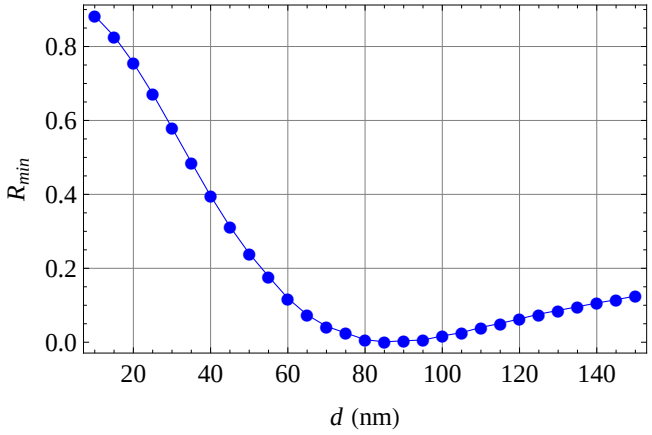

Fig. 10.19. Effect of groove depth on the reflectivity minimum, R_{min}, at resonance for a sinusoidal gold grating with a 1 μm period at a wavelength of 700 nm as a function of groove depth, d. When the minimum is zero, for a groove depth near 60 nm, all of the incident light is coupled into excitation of the SP.

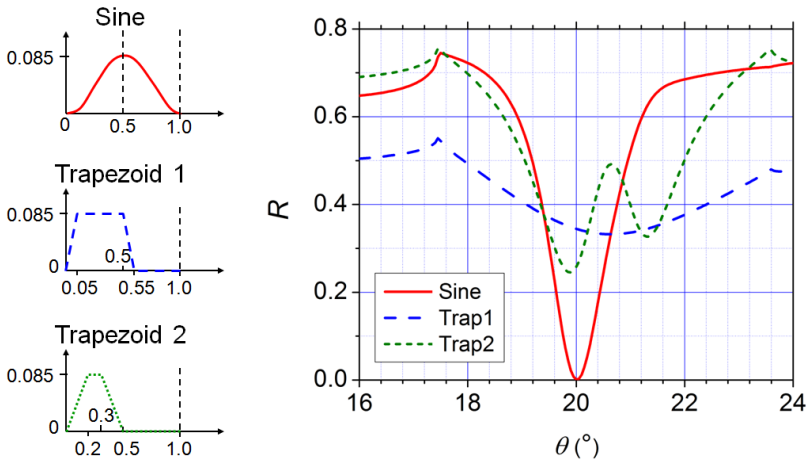

Fig. 10.20. Effect on the reflectivity of varying the shape of the groove profile.

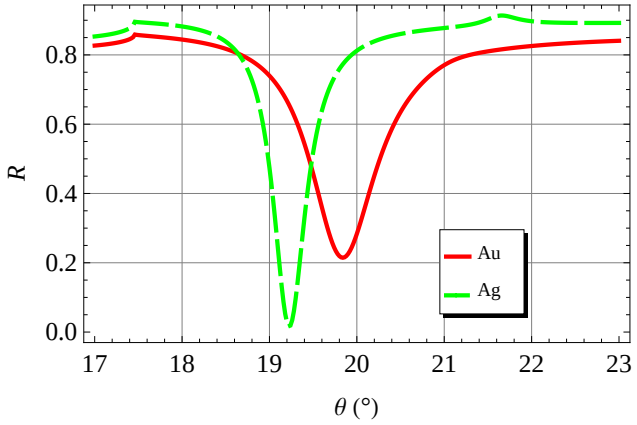

Fig. 10.21. Reflectivity as a function of polar angle of the SP resonance for gold and silver gratings with a 1 μm period and a sinusoidal groove depth of 50 nm at a wavelength of 700 nm. The reflectivity peak/cusp occurs for both metals at an angle of 17.5°, while the Wood's anomaly or SP resonance occurs at larger angles which depend on the refractive index of the specific metal. (*Mathematica* simulation.)

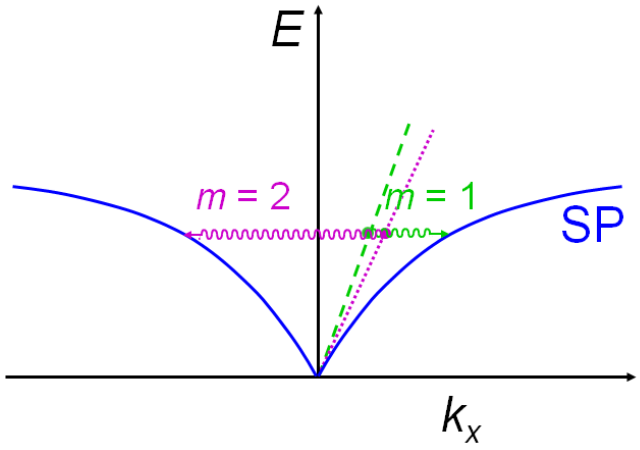

Fig. 10.22. Dispersion curve analysis which demonstrates how different angles of incidence can couple to different SPs. k_x is the component of the wavevector in the plane of the grating.

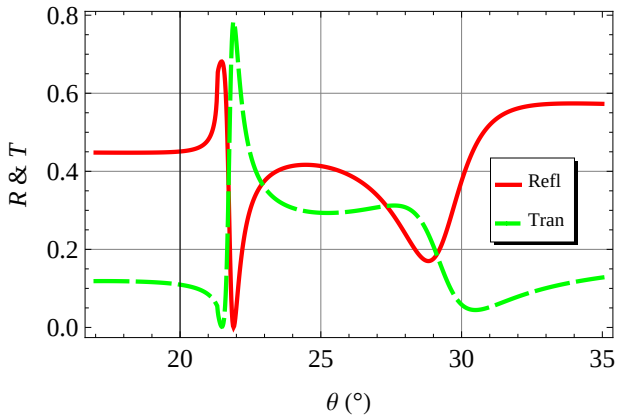

Fig. 10.23. Reflectivity and transmissivity calculated for a silver film that is 25 nm thick and corrugated with a sinusoidal grating with a 110 nm depth and 1.1 μm period at a wavelength of 700 nm. Two SP resonances are clearly observed in the reflectivity, at 22° and 29°, corresponding to symmetric and antisymmetric modes. (*Mathematica* simulation.)

10.6 End fire coupling

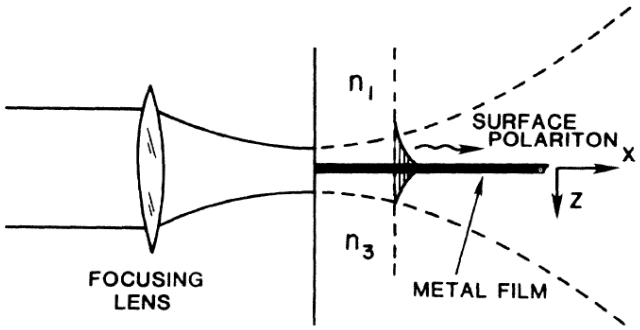

Fig. 10.24. End fire launching technique in which a laser beam is focused onto a thin metal film bounded by dielectrics on either side. Reprinted with permission from J. J. Burke, G. I. Stegeman and T. Tamir, *Phys. Rev. B* **33** 5186 (1986). © 1986 by the American Physical Society. [20]

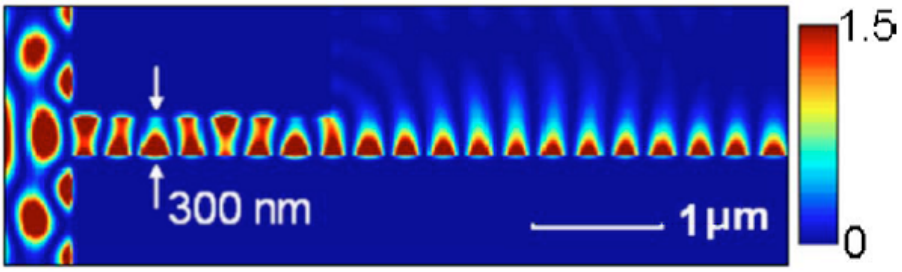

Fig. 10.25. FDTD calculation of optical energy transfer between two SP modes. A plane wave with free space wavelength of 600 nm is incident normally from the left upon a silver-air-silver waveguide with a 300 nm gap. The SP inside the waveguide propagates 2 μm through the waveguide and then reaches the air-silver planar surface. The $|H_z|^2$ intensity is plotted. Used by permission. [22]

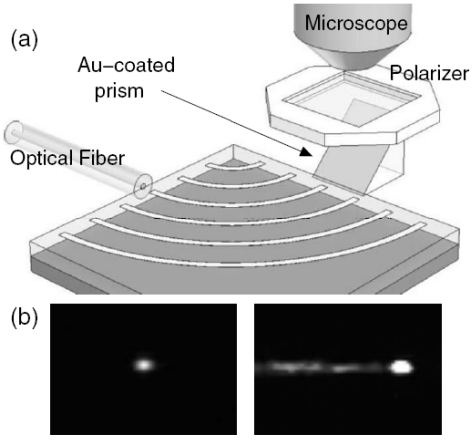

Fig. 10.26. (a) A PM fiber is used to bring light to the edge of a gold stripe waveguide at a free space wavelength of 1550 nm. The long-range SP excited by the light propagates around the stripe and is imaged at the other end by a microscope. (b) The left image is for a stripe with a 7.5 mm radius of curvature. The right image is for a 1 mm radius of curvature that has been overexposed to reveal the radiation losses along the curve. Reprinted with permission from A. Degiron, S-Y. Cho, C. Harrison, N. M. Jokerst, C. Dellagiacoma, O. J. F. Martin and D. R. Smith, *Phys. Rev. A* **77** 021804 (2008). © 2008 by the American Physical Society. [23]

10.7 Near field launching

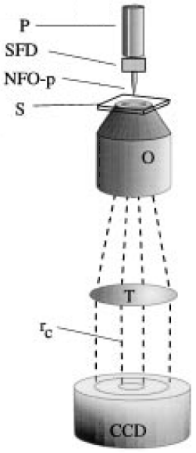

Fig. 10.27. Apparatus for launching SPs on a metallic film by a near field tapered fiber probe and observing the propagating SPs. Reprinted with permission from B. Hecht, H. Bielefeldt, L. Novotny, Y. Inouye, and D. W. Pohl, *Phys. Rev. Lett.* **77** 1889 (1996). © 1996 by the American Physical Society. [24]

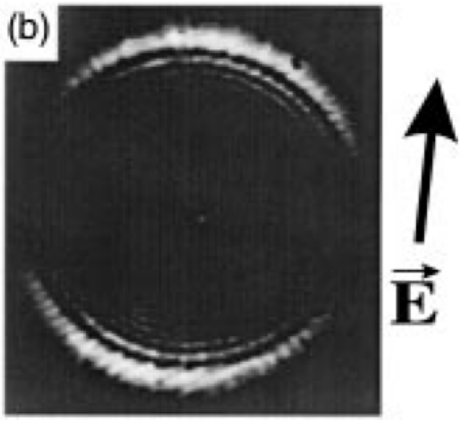

Fig. 10.28. Images obtained from the apparatus in Fig. 10.34 for a gold film at a free space wavelength of 514 nm. Reprinted with permission from B. Hecht, H. Bielefeldt, L. Novotny, Y. Inouye, and D. W. Pohl, *Phys. Rev. Lett.* **77** 1889 (1996). © 1996 by the American Physical Society. [24]

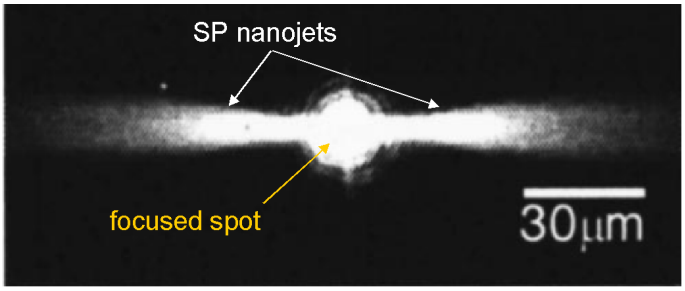

Fig. 10.29. SP jets excited by a beam of light focused onto a nanowire on a thin silver film. Reprinted with permission from H. Ditlbacher, J. R. Krenn, G. Schider, A. Leitner and F. R. Aussenegg, *Appl. Phys. Lett.* **81** #10, 1762 (2002) . © 2002, American Institute of Physics. [25]

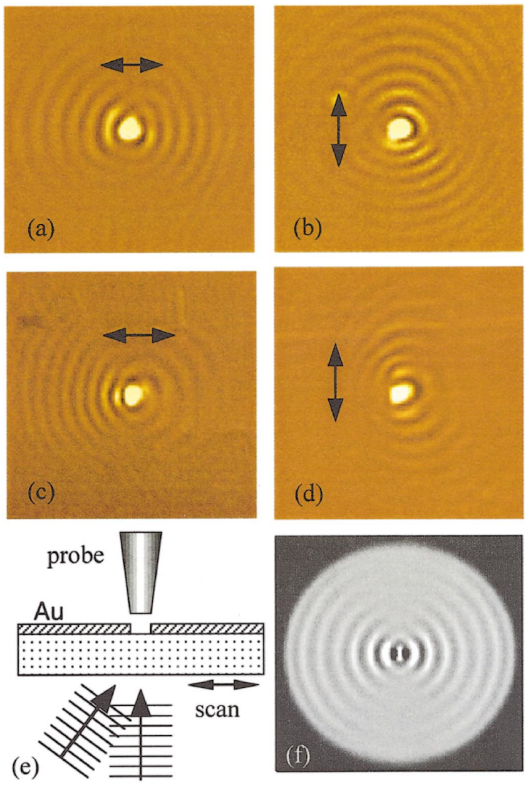

Fig. 10.30. SPs excited on a gold surface by light incident from the substrate at near normal incidence for (a) and (b) and at an inclined angle of incidence in (c) and (d) as shown in (d). The arrows in (a)-(d) indicate the direction of the incident polarization. (f) FDTD calculation of the normal component of the Poynting vector. Reprinted with permission from L. Yin, V. K. Vlasko-Vlasov, A. Rydh, J. Pearson, U. Welp, S.-H. Chang, S. K. Gray, G. C. Schatz, D. B. Brown and C. W. Kimball. Surface plasmons at single nanoholes in Au films. *Appl. Phys. Lett.* **85** (2004) 467. © 2004, American Institute of Physics. [26]

Appendix: description of grating code

In this section we discuss the Chandezon technique [31] for solving the vector diffraction of a plane wave incident upon a multilayer conformal thin film stack on a grating. As originally described, this technique was derived for conformal multilayer gratings, i.e., multilayer gratings of thin films in which the groove profile was conformal in each layer. A very useful enhancement of the technique was described by Priest *et al.* [32] for multilayer films with periodic grooves which are not conformal from layer to layer, and we include this enhancement in the discussion. Finally, the transfer matrix technique as originally used by Chandezon *et al.*, has been modified into a scattering matrix technique by Cotter *et al.* [33] in order to handle films which are exceptionally thick or grooves which are exceptionally deep without exceeding the numerical precision of conventional PC's. This option is also described and implemented.

We should also point out that rigorous vector diffraction theory has undergone an immense development in the last two decades by many research groups. Both the Chandezon technique and the other popular approach, the Fourier modal method, have been greatly improved and optimized for efficient computation of the diffracted fields. The following discussion is not meant to incorporate all of these improvements and advances, but to simply provide an introduction to the Chandezon technique so that the interested reader may more easily understand the literature.

10.5.1 Definition of groove profile

The basic geometry of the problem is shown in Fig. 10.31. As before, the grooves are parallel to the z axis and perpendicular to the x axis. The y axis is normal to the surface of the grating. The groove profile in each layer has a period d. The profile itself is allowed to vary from layer to layer, however. For the bottom of layer j the functional dependence of the groove profile is

$$y_j = d_j + a_j(x). \tag{10.1}$$

We choose $a(x=0) = 0$ for each layer, so

$$d_j = e_1 + e_2 + \cdots + e_{j-1} \tag{10.2}$$

with

$$d_0 = d_1 = 0. \tag{10.3}$$

Subscript 0 denotes the substrate and subscript Q+1 represents the upper dielectric for Q layers.

For the purposes of this implementation, we assume the groove profile in each layer is composed of piecewise continuous line segments with the same number of line segments and the same x coordinate end points as shown in Fig. 10.31. We should point out that the original Chandezon technique described here is more suited for a continuously differentiable groove profile. The piecewise linear groove profile generally requires a larger number of terms in the Fourier expansions to converge to an accurate result. This limitation has been removed by Plumey *et al.*, [34] but their work is beyond the scope of this discussion. Nevertheless, in practice even the groove profile shown in Fig. 10.31 is handled well by the Chandezon technique for the problems in which we are interested.

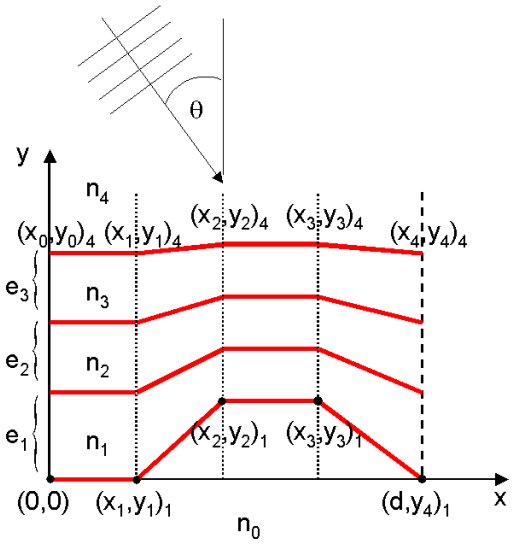

Fig. 10.31. Basic multilayer film stack for grating diffraction calculations. There is a semi-infinite substrate below (0,0) with refractive index n_0 and a semi-infinite dielectric medium above $(x_0, y_0)_{Q+1}$ with refractive index n_{Q+1} where there are Q thin films and Q+1 interfaces between layers. The groove profile in each layer is divided into L piecewise continuous line segments. In the example pictured, Q = 3 and L = 4. The incident plane wave lies in the xy plane and makes angle θ with the y axis.

By defining the groove profile in piecewise continuous line segments, the groove profile in each layer is specified by the set of L+1 line segment end points, $\{(0,0), (x_1, y_1), \ldots, (x_L, y_L)\}_j$ for the j^{th} layer. The thickness of the j^{th} layer at $x = 0$ is e_j. The n^{th} line segment for layer j is given by

$$a_{lj}(x) = \left(\frac{x - x_{l-1}^{j}}{x_l^j - x_{l-1}^{j}}\right)\left(y_l^j - y_{l-1}^{j}\right) + y_{l-1}^{j}. \tag{10.4}$$

The slope of this line segment is

$$\frac{\partial a_{lj}(x)}{\partial x} = a'_{lj} = \left(\frac{y_l^j - y_{l-1}^{j}}{x_l^j - x_{l-1}^{j}}\right). \tag{10.5}$$

The *change* in vertical distance between line segments is, in general, a function of x with period d,

$$\Delta_{lj}(x) \equiv\ a_{l,\,j+1}(x)\ -\ a_{l,\,j}(x). \tag{10.6}$$

If the films are conformal then $\Delta_j = 0$. We also define the derivative of this function,

$$\Delta'_{lj} =\ \frac{\partial}{\partial x}\left(a_{l,\,j+1}\ -\ a_{lj}\right) = a'_{l,\,j+1} - a'_{lj}. \tag{10.7}$$

Then

$$\Delta_{lj}(x) = \Delta'_{lj}\,x + \left[-\Delta'_{lj}\left(x_{l-1}^{j+1} - x_{l-1}^{j}\right) + \left(y_{l-1}^{j+1} - y_{l-1}^{j}\right)\right] \equiv \Delta'_{lj}\,x\ +\ f_{lj} \tag{10.8}$$

where we have explicitly exhibited the x dependence of Δ_{lj}.

The function $\exp\left(i\, r_q^j\, \Delta_j\right)$ also has period d and may be expanded in a Fourier series,

$$\exp\left[i\, r_q^j\, \Delta_j(x)\right] = \sum_{m=-\infty}^{\infty} L_m^j\left(r_q\right) \exp(i\, m\, K\, x) \tag{10.9}$$

where the grating vector is

$$K = \frac{2\,\pi}{d}, \tag{10.10}$$

and

$$\int_0^d \exp\left[i\, r_q^j\, \Delta_j(x)\right] \exp(-i\, n\, K\, x)\, dx =$$

$$\int_0^d \sum_m L_m^j\left(r_q\right) \exp(i\, m\, K\, x) \exp(-i\, n\, K\, x)\, dx$$

$$= \sum_m d\, L_m^j\left(r_q\right) \delta_{mn} = d\, L_n^j\left(r_q\right) \tag{10.12}$$

or

$$L_n^j\left(r_q\right) = \begin{cases} 1 & \text{for } \Delta_j = 0 \text{ and } n = 0 \\ 0 & \text{for } \Delta_j = 0 \text{ and } n \neq 0 \\ \frac{1}{d} \int_0^d \exp\left[i\, r_q^j\, \Delta_j(x) - i\, n\, K\, x\right] dx & \text{otherwise} \end{cases}. \tag{10.13}$$

Because Δ_j is segmented along the groove in our scheme, the integration in Eq. (10.13) is also a summation over each segment,

$$L_n^j\left(r_q\right) = \frac{1}{d} \sum_{l=1}^{L} \begin{cases} x_l - x_{l-1} & \text{for } \Delta_{lj} = 0 \text{ and } n = 0 \\ \int_{x_{l-1}}^{x_l} \exp\left[i\, r_q^j\, \Delta_{lj}(x) - i\, n\, K\, x\right] dx & \text{otherwise} \end{cases}. \tag{10.14}$$

The integration in Eq. (10.14) is easily carried out with Eq. (10.8).

For future reference, we define two additional functions for each layer, $C_j(x)$ and $D_j(x)$, which are also constant within each line segment of the groove profile,

$$C_{nj} = \frac{1}{1 + \left(a'_{nj}\right)^2} \tag{10.15}$$

and

$$D_{nj} = \frac{a'_{nj}}{1 + \left(a'_{nj}\right)^2}. \tag{10.16}$$

The functions $C_j(x)$ and $D_j(x)$ are periodic with the groove profile and can be expanded in Fourier series themselves. Specifically,

$$C_j(x) = \sum_{p=-N}^{N} c_{pj} \exp(i\, p\, K\, x) \tag{10.17}$$

and

$$D_j(x) = \sum_{p=-N}^{N} d_{pj} \exp(i\, p\, K\, x) \tag{10.18}$$

in the limit N → ∞, where

$$c_{pj} = \sum_{n=1}^{L} \begin{cases} \frac{C_{nj}\,(x_n - x_{n-1})}{d} & p = 0 \\ \frac{i C_{nj}}{2\pi\, p}[\exp(-i\, p\, K\, x_n) - \exp(-i\, p\, K\, x_{n-1})] & \text{otherwise} \end{cases}. \tag{10.19}$$

and

$$d_{pj} = \sum_{n=1}^{L} \begin{cases} \frac{D_{nj}\,(x_n - x_{n-1})}{d} & p = 0 \\ \frac{i D_{nj}}{2\pi\, p}[\exp(-i\, p\, K\, x_n) - \exp(-i\, p\, K\, x_{n-1})] & \text{otherwise} \end{cases}. \tag{10.20}$$

Eqs. (10.19) and (10.20) are easily derived from the Fourier integral. For example, Eq. (10.11) follows from Eq. (10.10) by

$$\int_0^d C_j(x) \exp(-i\, q\, K\, x)\, dx = \sum_{p=-N}^{N} \int_0^d c_{pj} \exp(i\, p\, K\, x) \exp(-i\, q\, K\, x)\, dx \tag{10.21}$$

$$= \sum_{p=-N}^{N} \left(d\, \delta_{pq}\right) c_{pj} = d\, c_{qj}. \tag{10.22}$$

By Eq. (10.13), $C_j(x)$ is piecewise constant, so Eq. (10.17) can be rewritten as

$$d\,c_{qj} = \sum_{n=1}^{L} C_{nj} \int_{x_{n-1}}^{x_n} \exp(-i\,q\,K\,x)\,dx \tag{10.23}$$

or, with the substitution $q \to p$ we arrive at Eq. (10.19), and similarly for d_{pj}.

To recap, in order to compute the Fourier coefficients c_{pj} and d_{pj} of the functions C_j and D_j we follow the following procedure. First, for each layer j, we compute the slopes, a'_{nj}, for each line segment in the groove profile according to Eq. (10.5). From Eqs. (10.15) and (10.16) we compute the coefficients C_{nj} and D_{nj} for each line segment n within layer j. Finally, from Eqs. (10.19) and (10.20), the Fourier coefficients c_{pj} and d_{pj} of the functions C_j and D_j, respectively, are obtained.

We also note that for sinusoidal groove profiles, analytical expressions can be obtained for c_{pj}, d_{pj}, and $L_n^j(r_q)$ as described by L. Li. [35]

10.5.2 Coordinate system transformation

The next step is to define the fields everywhere. One of the clever aspects of Chandezon's technique is the use of coordinate transforms so that the groove profiles are planar surfaces in the new coordinate systems. Another clever idea is to represent the reflected propagating (diffracted) fields in the upper dielectric medium as a Fourier plane wave expansion everywhere above the top interface, even inside the grooves where such an expansion is not physically correct, and to then define the *total* field in the upper medium as a sum of the propagating modes and evanescent modes, the latter of which are chosen to provide the total true field even within the grooves.

The incident field is a plane wave with wavevector k_i and polar angle of incidence θ in the xy plane as shown in Fig. 10.31,

$$F^i = \exp(i\mathrm{k}_i\,x\sin\theta - i\mathrm{k}_i\,y\cos\theta). \tag{10.24}$$

The reflected, plane wave **propagating** modes are given by the expansion

$$F^r = \sum_{n\in U_r} B_n^r \exp(i\,\alpha_n\,x + i\,\beta_n\,y). \tag{10.25}$$

We will assume that there are P_r of these modes, each with unknown amplitude B_n^r. The transmitted plane wave **propagating** modes are given by the expansion

$$F^t = \sum_{n \in U_t} B_n^t \exp(i\,\alpha_n\,x - i\,\beta_n\,y) \tag{10.26}$$

and we assume that there are P_t of these modes with unknown amplitudes B_n^t. The α_n are the wavevector components along the x-direction of the various diffracted orders,

$$\alpha_n = k_i \sin\theta + n\,K, \tag{10.27}$$

and the β_n are the wavevector components along the y-direction of the various diffracted orders,

$$\beta_n^j = \sqrt{k_j^2 - \alpha_n^2} = \sqrt{\epsilon_j\,k_0^2 - \alpha_n^2} \quad \text{for} \quad k_i \geq |\alpha_n|,\ i.e.,\ n \in U_{r,t}. \tag{10.28}$$

ϵ_j is the relative permittivity (dielectric constant) of layer j, and k_0 is the vacuum wavevector previously defined. α_n is the same for each layer of the film stack as well as the upper dielectric and the substrate by virtue of Snell's law. However, β_n^j is a function of the index of refraction and in general will be different for each layer, the upper dielectric, and the substate. For that reason it is given the superscript j. When $n \notin U_{r,t}$, $k_i < |\alpha_n|$, then β_n is imaginary and the fields in the expansions, Eqs. (10.25) and (10.26), are evanescent. When the total fields in the upper dielectric and/or the substrate are expressed by this expansion of real and evanescent orders, this is the well known Raleigh approximation for the diffracted fields. Unfortunately, this expansion does not correctly reproduce the fields *within* the groove region and, therefore, fails when the grooves have any appreciable depth. [36]

In the Chandezon technique the evanescent fields in the upper dielectric and the substrate are computed in the transformed coordinate system to properly represent the total field in this region. There is a separate coordinate system for each layer in the film stack, but for now we will not include the layer label j and consider a generic transformed coordinate system. Following the standard notation in the literature, the axes of the transformed coordinate system are labelled v, u, and w where

$$v = x, \qquad u_j = y - a_j(x) \qquad \text{and} \qquad w = z. \tag{10.29}$$

In the transformed coordinate system it is convenient to define two different sets of basis vectors (which are not all unit vectors) in terms of the standard Cartesian coordinate system basis vectors. One set is represented by subscripts,

$$\vec{\boldsymbol{e}}_1 = \hat{\boldsymbol{i}} + a'\,\hat{\boldsymbol{j}} \qquad \vec{\boldsymbol{e}}_2 = \hat{\boldsymbol{j}}, \qquad \text{and} \qquad \vec{\boldsymbol{e}}_3 = \hat{\boldsymbol{k}} \tag{10.30}$$

and the other by superscripts,

$$\vec{\hat{e}}^1 = \hat{i}, \qquad \vec{\hat{e}}^2 = \hat{j} - a' \hat{i}, \quad \text{and} \qquad \vec{\hat{e}}^3 = \hat{k}. \tag{10.31}$$

The basis vector $\hat{e}_1$ is parallel to the surface of the groove profile and is, therefore, useful for computing the tangential components of the field vectors at the interfaces, while the $\vec{\hat{e}}^2$ basis vector is normal to the surface of the groove profile and is useful for computing the normal components of the field vectors at the interfaces. There are several useful relationships between the two sets of basis vectors,

$$\vec{\hat{e}}^i \cdot \vec{\hat{e}}_j = \delta_{ij}, \qquad \hat{e}^i \times \vec{\hat{e}}_j = e_{ijk} \vec{\hat{e}}_k \quad \text{and} \quad \vec{\hat{e}}_i \times \vec{\hat{e}}_j = e_{ijk} \vec{\hat{e}}^k \tag{10.32}$$

where δ_{ij} is the Kronecker delta function and e_{ijk} is Levi-Civita symbol or permutation symbol defined by

$$e_{ijk} = \begin{cases} 0 & \text{for } i = j,\ i = k,\ \text{or } j = k \\ +1 & \text{for } (1, 2, 3),\ (2, 3, 1),\ \text{or } (3, 1, 2) \\ -1 & \text{for } (1, 3, 2),\ (3, 2, 1),\ \text{or } (2, 1, 3). \end{cases} \tag{10.33}$$

Any vector $\vec{A}$ can be written

$$\vec{A} = A_v \vec{\hat{e}}_1 + A_u \vec{\hat{e}}_2 + A_w \vec{\hat{e}}_3 = A^1 \vec{\hat{e}}_1 + A^2 \vec{\hat{e}}_2 + A^3 \vec{\hat{e}}_3. \tag{10.34}$$

The tangential components of the vector $\vec{A}$ at an interface are

$$\hat{e}_1 \cdot \vec{A} = \frac{\vec{\hat{e}}_1}{\sqrt{1 + (a')^2}} \cdot \vec{A} = \frac{A^1}{\sqrt{1 + (a')^2}} \tag{10.35}$$

and

$$\hat{e}_3 \cdot \vec{A} = A^3. \tag{10.36}$$

The normal component of the vector $\vec{A}$ at an interface is

$$\hat{e}^2 \cdot \vec{A} = \frac{\vec{e}^2}{\sqrt{1+(a')^2}} \cdot \vec{A} = \frac{A_u}{\sqrt{1+(a')^2}}. \tag{10.37}$$

The vector component A^2 can be represented in terms of the subscript basis vectors by

$$A^2 = \left(\left(\vec{A} - A^1 \vec{e}^1 - A^3 \vec{e}^3\right) \cdot \vec{e}_2\right) \Big/ \left(1+(a')^2\right) = \left(\left(A_v \vec{e}_1 + A_u \vec{e}_2 + A_w \vec{e}_3\right) \cdot \vec{e}^2\right) \Big/ \left(1+(a')^2\right) - \frac{A^1 \vec{e}^1 \cdot \vec{e}^2}{1+(a')^2} \tag{10.38}$$

$$= \frac{A_u}{1+(a')^2} + \frac{a' A^1}{1+(a')^2} = C A_u + D A^1 \tag{10.39}$$

where C and D are the functions previously defined in Eqs. (10.15) and (10.18). Similarly,

$$A_v = \left(\left(\vec{A} - A_u \vec{e}_2 - A_w \vec{e}_3\right) \cdot \vec{e}_1\right) \Big/ \left(1+(a')^2\right) = \left(\left(A^1 \vec{e}^1 + A^2 \vec{e}^2 + A^3 \vec{e}^3\right) \cdot \vec{e}_1\right) \Big/ \left(1+(a')^2\right) = \frac{A^1}{1+(a')^2} - \frac{a' A_u}{1+(a')^2} = C A^1 - D A_u \tag{10.40}$$

and

$$A_w = \left(\vec{A} - A_v \vec{e}_1 - A_u \vec{e}_2\right) \cdot \vec{e}_3 = \left(A^1 \vec{e}^1 + A^2 \vec{e}^2 + A^3 \vec{e}^3\right) \cdot \vec{e}_3 = A^3. \tag{10.41}$$

The differential operator is

$$\nabla = \left(\frac{\partial}{\partial v}\right)\vec{\boldsymbol{e}}^1 + \left(\frac{\partial}{\partial u}\right)\vec{\boldsymbol{e}}^2 + \left(\frac{\partial}{\partial w}\right)\vec{\boldsymbol{e}}^3 \tag{10.42}$$

so the curl of a vector is

$$\nabla \times \vec{\boldsymbol{A}} = \left(\frac{\partial A^3}{\partial u} - \frac{\partial A^2}{\partial w}\right)\vec{\boldsymbol{e}}_1 + \left(\frac{\partial A^1}{\partial w} - \frac{\partial A^3}{\partial v}\right)\vec{\boldsymbol{e}}_2 + \left(\frac{\partial A^2}{\partial v} - \frac{\partial A^1}{\partial u}\right)\vec{\boldsymbol{e}}_3. \tag{10.43}$$

By combining Eq. (10.39) with Eq. (10.43), we can separate the component parts of the Maxwell-like equation,

$$\nabla \times \vec{\boldsymbol{A}} = \boldsymbol{i}\,\boldsymbol{\gamma}\,\vec{\boldsymbol{R}} \tag{10.44}$$

into

$$\left(\frac{\partial A^3}{\partial u} - \frac{\partial A^2}{\partial w}\right) = \frac{\partial A^3}{\partial u} - \frac{\partial\left(C\,A_u + D\,A^1\right)}{\partial w} = i\,\gamma\,R_v = i\,\gamma\left(C\,R^1 - D\,R_u\right), \tag{10.45}$$

$$\left(\frac{\partial A^1}{\partial w} - \frac{\partial A^3}{\partial v}\right) = i\,\gamma\,R_u, \tag{10.46}$$

and

$$\left(\frac{\partial A^2}{\partial v} - \frac{\partial A^1}{\partial u}\right) = \frac{\partial\left(C\,A_u + D\,A^1\right)}{\partial v} - \frac{\partial A^1}{\partial u} = i\,\gamma\,R_w = i\,\gamma\,R^3. \tag{10.47}$$

10.5.3 Solution of Maxwell's equations within each layer

Maxwell's equations are

$$\nabla \times \vec{\boldsymbol{E}} = \; i\,\gamma_1\,\vec{\boldsymbol{H}} \tag{10.48}$$

and

$$\nabla \times \vec{\boldsymbol{H}} = \; -i\,\gamma_2\,\vec{\boldsymbol{E}} \tag{10.49}$$

where

$$\gamma_1 = \frac{\omega\, Z_0}{c}\,\mu_r = \; k_0\, Z_0\, \mu_r, \tag{10.50}$$

$$\gamma_2 = \frac{\omega}{Z_0\, c}\,\epsilon_r \; = \; \frac{k_0}{Z_0}\,\epsilon_r, \tag{10.51}$$

and

$$Z_0 \equiv \sqrt{\frac{\mu_0}{\epsilon_0}}\,. \tag{10.52}$$

μ_r and ϵ_r are the relative permeability and permittivity of the material in a given layer, respectively, and μ_0 and ϵ_0 are the permeability and permittivity of free space, respectively.

When the incident light is in the *xy* plane, Maxwell's equations can be reduced to three coupled equations for the TE and TM modes separately. Specifically, we define new fields $\vec{\boldsymbol{F}}$ and $\vec{\boldsymbol{G}}$ where

$$\vec{\boldsymbol{F}} \equiv \vec{\boldsymbol{E}} \qquad \text{and} \qquad \vec{\boldsymbol{G}} \equiv \gamma_1\,\vec{\boldsymbol{H}} \quad \text{for the TE mode, and} \tag{10.53}$$

$$\vec{\boldsymbol{F}} \equiv Z_0\,\vec{\boldsymbol{H}} \qquad \text{and} \qquad \vec{\boldsymbol{G}} \equiv -Z_0\,\gamma_2\,\vec{\boldsymbol{E}} \quad \text{for the TM mode.} \tag{10.54}$$

Therefore, the *F* field has components along the *w* (*z*) axis, so F_v, F_u, F^1, and F^2 are all zero, while the *G* field has components in the *uv* (*xy*) plane of incidence, so G_w and G^3 are zero. Then Maxwell's equations for both modes can be expressed by two equations,

$$\nabla \times \vec{\boldsymbol{F}} = i\,\vec{\boldsymbol{G}} \tag{10.55}$$

and

$$\nabla \times \vec{\boldsymbol{G}} = -i\,\boldsymbol{\gamma}_1\,\boldsymbol{\gamma}_2\,\vec{\boldsymbol{F}}. \tag{10.56}$$

Due to the symmetry of the problem, there is no *w* dependence of the fields. From Eqs. (10.45) - (10.47), we have

$$\frac{\partial F^3}{\partial u} = i\left(C\,G^1 - D\,G_u\right), \tag{10.57}$$

$$i\,\frac{\partial F^3}{\partial v} = G_u, \tag{10.58}$$

and

$$\frac{\partial\left(C\,G_u + D\,G^1\right)}{\partial v} - \frac{\partial G^1}{\partial u} = -i\,\gamma_1\,\gamma_2\,F^3. \tag{10.59}$$

We eliminate G_u from Eqs. (10.57) and (10.59) using Eq. (10.58), and then simplify the notation by letting $F^3 \to F$ and $G^1 \to G$. Maxwell's equations have now been reduced to two linear differential equations which define the fields within each layer of the film stack,

$$\frac{\partial F}{\partial u} = i\,C\,G + D\,\frac{\partial F}{\partial v} \tag{10.60}$$

and

$$\frac{\partial G}{\partial u} = i\,\gamma_1\,\gamma_2\,F + \frac{\partial}{\partial v}\left(i\,C\,\frac{\partial F}{\partial v}\right) + \frac{\partial (D\,G)}{\partial v}. \tag{10.61}$$

To solve these equations, we recall that the C and D functions have been expanded in a Fourier series in Eqs. (10.17) and (10.18) in the variable $v = x$. We rewrite those equations and their partial derivatives with respect to *v*.

$$C_j(v) = \sum_p c_{pj} \exp(i\,p\,K\,v) \tag{10.62}$$

$$\frac{\partial C_j(v)}{\partial v} = \sum_p i\, p\, K\, c_{pj} \exp(i\, p\, K\, v) \tag{10.63}$$

$$D_j(v) = \sum_p d_{pj} \exp(i\, p\, K\, v) \tag{10.64}$$

and

$$\frac{\partial D_j(v)}{\partial v} = \sum_p i\, p\, K\, d_{pj} \exp(i\, p\, K\, v). \tag{10.65}$$

The fields F and G and their partial derivatives are also expanded in Fourier series in v. The layer variable j is explicitly exhibited.

$$F^j(u, v) = \sum_m F_m^j(u) \exp(i\, \alpha_m\, v) \tag{10.66}$$

$$\frac{\partial F^j(u, v)}{\partial v} = \sum_m i\, \alpha_m\, F_m^j(u) \exp(i\, \alpha_m\, v) \tag{10.67}$$

$$G^j(u, v) = \sum_m G_m^j(u) \exp(i\, \alpha_m\, v) \tag{10.68}$$

$$\frac{\partial G^j(u, v)}{\partial v} = \sum_m i\, \alpha_m\, G_m^j(u) \exp(i\, \alpha_m\, v) \tag{10.69}$$

The Fourier coefficients F_m and G_m are the field amplitudes in the transformed coordinate system within each layer. Entering Eqs. (10.62) - (10.69) into Eq. (10.60) gives

$$\frac{\partial F^j(u, v)}{\partial u} = i \sum_{m,p} \left(c_{pj}\, G_m^j + \alpha_m\, d_{pj}\, F_m^j\right) \exp\left(i\, \alpha_{m+p}\, v\right) \tag{10.70}$$

since

$$\alpha_m + p\, K = (k_i \sin\theta + m\, K) + p\, K = \alpha_{m+p}. \tag{10.71}$$

Substituting $m \to m - p$, we can eliminate the v dependence and obtain an equation for each Fourier component of the field F,

$$\frac{\partial F_m^j(u)}{\partial u} = i \sum_p \left(c_{pj}\, G_{m-p}^j + \alpha_{m-p}\, d_{pj}\, F_{m-p}^j\right). \tag{10.72}$$

Finally, we let $p \to m - p$,

$$\frac{\partial F_m^j(u)}{\partial u} = i \sum_p \left(c_{m-p,j}\, G_p^j + \alpha_p\, d_{m-p,j}\, F_p^j\right). \tag{10.73}$$

With Eqs. (10.64), (10.65), (10.68) and (10.69) we find

$$\frac{\partial (D\, G)}{\partial v} = \frac{\partial D}{\partial v}\, G + D\, \frac{\partial G}{\partial v} \tag{10.74}$$

$$\begin{aligned} = \; & i \sum_p i\, p\, K\, d_{pj} \exp(i\, p\, K\, v) \cdot \sum_m G_m^j(u) \exp(i\, \alpha_m\, v) + \\ & i \sum_p d_{pj} \exp(i\, p\, K\, v) \cdot \sum_m \alpha_m\, G_m^j(u) \exp(i\, \alpha_m\, v) \end{aligned} \tag{10.75}$$

$$= i \sum_{m,p} (p\, K + \alpha_m)\, d_{pj}\, G_m^j \exp\left(i\, \alpha_{m+p}\, v\right) \tag{10.76}$$

$$= i \sum_{m,p} \alpha_{m+p}\, d_{pj}\, G_m^j \exp\left(i\, \alpha_{m+p}\, v\right) \tag{10.77}$$

$$= i \sum_{m,p} \alpha_m\, d_{pj}\, G_{m-p}^j \exp(i\, \alpha_m\, v) \tag{10.78}$$

where in the last step we have again made the substitution $m \to m - p$.

Also, Eqs. (10.62), (10.63), (10.66), and (10.67) give

$$\frac{\partial}{\partial v}\left(i\,C\,\frac{\partial F}{\partial v}\right) = i\,\frac{\partial C}{\partial v}\cdot\frac{\partial F}{\partial v} + i\,C\,\frac{\partial^2 F}{\partial v^2} \tag{10.79}$$

$$= \; i\sum_p i\,p\,K\,c_{pj}\exp(i\,p\,K\,v)\cdot\sum_m i\,\alpha_m\,F_m^j(u)\exp(i\,\alpha_m\,v)\; - \tag{10.80}$$

$$i\sum_p c_{pj}\exp(i\,p\,K\,v)\cdot\sum_m \alpha_m^2\,F_m^j(u)\exp(i\,\alpha_m\,v) \tag{10.81}$$

$$= \; -i\sum_{m,p}\alpha_m\,(p\,K\,+\,\alpha_m)\,c_{pj}\,F_m^j\exp\left(i\,\alpha_{m+p}\,v\right) \tag{10.82}$$

$$= \; -i\sum_{m,p}\alpha_m\,\alpha_{m+p}\,c_{pj}\,F_m^j\exp\left(i\,\alpha_{m+p}\,v\right) \tag{10.83}$$

$$= \; -i\sum_{m,p}\alpha_{m-p}\,\alpha_m\,c_{pj}\,F_{m-p}^j\exp(i\,\alpha_m\,v) \tag{10.84}$$

Using Eqs. (10.78) and (10.84) in Eq. (10.61) gives

$$\frac{\partial G^j}{\partial u} = i\left(\sum_{m,p}\left[\gamma_1^j\,\gamma_2^j\,\delta_{mp}\,F_p^j\right] + \sum_{m,p}\left[-\alpha_{m-p}\,\alpha_m\,c_{pj}\,F_{m-p}^j + \alpha_m\,d_{pj}\,G_{m-p}^j\right]\right)\exp(i\,\alpha_m\,v). \tag{10.85}$$

In the second summation, we make the substitution $p \to m - p$,

$$\frac{\partial G^j(u,v)}{\partial u} = i\left(\sum_{m,p}\left[\gamma_1^j\,\gamma_2^j\,\delta_{mp}\,F_p^j\right] + \sum_{m,p}\left[-\alpha_p\,\alpha_m\,c_{m-p,j}\,F_p^j + \alpha_m\,d_{m-p,j}\,G_p^j\right]\right)\exp(i\,\alpha_m\,v), \tag{10.86}$$

and then combine the summations and pick out the terms of the individual Fourier components of G^j,

$$\frac{\partial G_m^j(u)}{\partial u} = i \sum_p \left[\left(\gamma_1^j \gamma_2^j \delta_{mp} - \alpha_p \alpha_m c_{m-p,j} \right) F_p^j + \alpha_m d_{m-p,j} G_p^j \right]. \tag{10.87}$$

Eqs. (10.73) and (10.87) are an infinite set of linear differential equations in the field components. To satisfy these equations, the u dependence of the field components F_m and G_m must clearly be exponential. These two sets of equations can be put into the form of a linear partial differential vector equation. Specifically, we let the F_m and G_m field amplitudes of the various Fourier components in layer j, where $-N \le m \le +N$, be represented by the vector $\vec{\zeta}^j$ with 4N+2 components,

$$\vec{\zeta}^j(u) \equiv \left\{ F_{-N}^j, \ ...., F_{+N}^j, G_{-N}^j, \ ...., G_{+N}^j \right\} \tag{10.88}$$

where in principle $N \to \infty$, but in practice we truncate N at a sufficiently large number to achieve the desired accuracy in the calculation. Eqs. (10.73) and (10.87) can be written as a matrix equation,

$$-i \frac{\partial \vec{\zeta}^j}{\partial u} = \begin{pmatrix} \tilde{\mathbf{A}}^j & \tilde{\mathbf{B}}^j \\ \tilde{\mathbf{C}}^j & \tilde{\mathbf{D}}^j \end{pmatrix} \vec{\zeta}^j \tag{10.89}$$

where $\tilde{\mathbf{A}}$, $\tilde{\mathbf{B}}$, $\tilde{\mathbf{C}}$, and $\tilde{\mathbf{D}}$ are rank 2N+1 square matrices with components given by,

$$A_{mn}^j = \alpha_n d_{m-n,j} \tag{10.90}$$

$$B_{mn}^j = c_{m-n,j} \tag{10.91}$$

$$C_{mn}^j = \gamma_1^j \gamma_2^j \delta_{mn} - \alpha_m \alpha_n c_{m-n,j} \tag{10.92}$$

and

$$D_{mn}^j = \alpha_m d_{m-n,j}. \tag{10.93}$$

The indices *m* and *n* range between -N and +N.

When we consider the boundary conditions at the interfaces between layers in the next section, we will find that it is easier work with modified fields within each layer, $\hat{F}$ and $\hat{G}$. First of all, we define the new variable η_j,

$$\eta_j \equiv \begin{cases} \frac{1}{\mu_r} & \text{for the TE mode} \\ \\ \frac{1}{\epsilon_r} & \text{for the TM mode.} \end{cases} \tag{10.94}$$

Then

$$\hat{F}_m \equiv F_m \tag{10.95}$$

and

$$\hat{G}_m \equiv \eta_j G^1_m. \tag{10.96}$$

In terms of the new fields, the vector

$$\vec{\hat{\boldsymbol{\zeta}}}^{\,j}(u) \equiv \left\{\hat{F}_{-N}, \ ...., \hat{F}_{+N}, \hat{G}_{-N}, \ ...., \hat{G}_{+N}\right\} \tag{10.97}$$

is a solution of the linear partial differential equation

$$-i\,\frac{\partial \vec{\hat{\boldsymbol{\zeta}}}^{\,j}}{\partial u} = \begin{pmatrix} \tilde{\mathbf{A}}^{\,j} & \frac{\tilde{\mathbf{B}}^{\,j}}{\eta_j} \\ \\ \eta_j\,\tilde{\mathbf{C}}^{\,j} & \tilde{\mathbf{D}}^{\,j} \end{pmatrix} \vec{\hat{\boldsymbol{\zeta}}}^{\,j} \equiv \tilde{\mathbf{T}}\,\vec{\hat{\boldsymbol{\zeta}}}^{\,j}. \tag{10.98}$$

(The caret on top of this vector is the standard notation used in the literature, but *does not* indicate that this is a unit vector, which it is not). $\tilde{\mathbf{T}}$ is a rank 4N+2 square matrix, and there are 4N+2 independent solutions to Eq. (10.98), indexed by *q*, of the form

$$\vec{\hat{\boldsymbol{\zeta}}}^{\,j}(u) = \vec{\hat{\boldsymbol{\zeta}}}^{\,j}_q \exp\left(i\,r^j_q\,u\right). \tag{10.99}$$

The vector amplitudes $\vec{\hat{\zeta}}_q^{\,j}$ of these independent solutions of the fields which can exist in each layer are fixed by matching boundary conditions. Once the boundary conditions have been applied, the total field within each layer is a sum of these q solutions with appropriate weighting amplitudes. Plugging Eq. (10.99) into Eq. (10.98) gives

$$-i\,\frac{\partial \vec{\hat{\zeta}}^{\,j}(u)}{\partial u} = r_q^j\,\vec{\hat{\zeta}}_q^{\,j}\exp\left(i\,r_q^j\,u\right) = r_q^j\,\vec{\hat{\zeta}}^{\,j} = \tilde{\mathbf{T}}^j\,\vec{\hat{\zeta}}^{\,j}, \tag{10.100}$$

so we see that the constants r_q are simply the eigenvalues of the matrix $\tilde{\mathbf{T}}$, and the $\vec{\hat{\zeta}}_q^{\,j}$ are vectors proportional to the eigenvectors of $\tilde{\mathbf{T}}$. The eigenvalues, r_q, determine whether or not the modes corresponding to each vector $\vec{\hat{\zeta}}_q$ are evanescent or propagating. If the former, then the r_q value determines if the field decays exponentially in the upward or downward direction. If the latter, the r_q value determines if the field is propagating in the upward or downward direction. There will be 2N+1 eigenvalues for which $\mathrm{Re}\left(r_q\right) > 0$ (some propagating and some evanescent modes), and 2N+1 eigenvalues for which $\mathrm{Re}\left(r_q\right) < 0$. For propagating modes, $\mathrm{Im}\left(r_q\right) = 0$. If, in addition, $\mathrm{Re}\left(r_q\right) > 0$, then the modes are propagating in the upward direction (we assume an exp(-$i\omega$t) time dependence for the fields). Likewise, $\mathrm{Re}\left(r_q\right) < 0$ with $\mathrm{Im}\left(r_q\right) = 0$ corresponds to a downward propagating mode. If $\mathrm{Im}\left(r_q\right) \neq 0$, then the modes either grow or decay exponentially in the vertical direction. If $\mathrm{Im}\left(r_q\right) > 0$, then the modes decay exponentially as u (or y) $\to \infty$. If $\mathrm{Im}\left(r_q\right) < 0$, then the modes decay exponentially as u (or y) $\to -\infty$.

Let $\hat{\mathbf{V}}$ be the complete set of normalized eigenvectors of $\tilde{\mathbf{T}}$. Then

$$\vec{\hat{\zeta}}_q^{\,j} = b_q^j\,\hat{\mathbf{V}}_q^j \tag{10.101}$$

where the b_q^j are the 4N+2 (as yet unknown) constants of proportionality. The complete solution to Eq. (10.100) is

$$\vec{\hat{\zeta}}^{\,j}(u) = \sum_q \vec{\hat{\zeta}}_q^{\,j}\exp\left(i\,r_q^j\,u\right) = \sum_q b_q^j\,\hat{\mathbf{V}}_q^j\exp\left(i\,r_q^j\,u\right). \tag{10.102}$$

Each separate diffraction order within a layer is given by one component of the vector sum $\vec{\hat{\boldsymbol{\zeta}}}^{\,j}(u)$ on the left hand side of this equation. For example, if N = 2 and we are interested in the amplitude of $+1^{st}$ diffracted order of the TE mode, then from Eqs. (10.55) and (10.95) - (10.97),

$$\vec{\hat{\boldsymbol{\zeta}}}^{\,j}(u) \equiv \{E_{-2}, E_{-1}, E_0, E_{+1}, E_{+2}, \eta_j \gamma_1 H_{-2}, \eta_j \gamma_1 H_{-1}, \eta_j \gamma_1 H_0, \eta_j \gamma_1 H_{+1}, \eta_j \gamma_1 H_{+2}\} \tag{10.103}$$

so we need to solve for the fourth component of $\vec{\hat{\boldsymbol{\zeta}}}^{\,j}$ which is itself a sum of the fourth components of the 4N+2 eigenvectors $\hat{\mathbf{V}}_q^j$ weighted by $b_q^j \exp(i\, r_q^j\, u)$. For convenience we follow the procedure of Priest *et al.* [32] and multiply each term in the sum by the phase factor $\exp(-i\, r_q^j\, d_j)$ and include the reciprocal factor in the values for b_q^j in order to fix the phase to zero at the bottom interface of layer *j*.

If we now define a new square matrix $\tilde{\boldsymbol{M}}^j$ of rank 4N+2 whose columns are composed of the eigenvectors $\hat{\mathbf{V}}_q^j$, and a new vector $\vec{\boldsymbol{b}}^j$ of the corresponding eigenvalues b_q^j then Eq. (10.102) can be written as a matrix equation,

$$\vec{\hat{\zeta}}^{\,j}(u) = \tilde{\mathrm{M}}^j\, \tilde{\boldsymbol{\Phi}}^j(u)\, \vec{\boldsymbol{b}}^j \tag{10.104}$$

or

$$\hat{\zeta}_p^j(u) = \sum_q M_{pq}^j \exp\left[i\, r_q^j\, (u - d_j)\right] b_q^j \tag{10.105}$$

where $\tilde{\boldsymbol{\Phi}}^j$ is a diagonal matrix incorporating the phase factors,

$$\Phi_{mq}^j(u) = \delta_{mq} \exp\left[i\, r_q\, (u - d_j)\right] = \delta_{mq} \exp(i\, r_q\, e_j) \exp(i\, r_q\, \Delta_j) \equiv \Gamma_{mq}^j \exp(i\, r_q\, \Delta_j). \tag{10.106}$$

The unknown b_q^j eigenvalue amplitudes are determined by matching boundary conditions at the interfaces between layers. At the bottom interface of layer *j*, $\tilde{\Phi}^j(d_j) = \tilde{\boldsymbol{I}}$, the identity matrix. Also, for the fields within the substrate (*j* = 0), the phase matrix at the interface with the bottom of the thin film stack is the identity matrix by definition. For the *top* interface of layer *j*,

$$y = d_{j+1} + a_{j+1}(x) \tag{10.107}$$

or

$$u_j = y - a_j(x) = d_{j+1} + \Delta_j(x), \tag{10.108}$$

so

$$\Phi^j_{mq}\left(d_{j+1} + \Delta_j(x)\right) = \delta_{mq} \exp\left(i\, r_q\, e_j\right) \exp\left(i\, r_q\, \Delta_j(x)\right). \tag{10.109}$$

We note that in general Δ_j is a periodic function of x. When the films are conformal, $\Delta = 0$ and

$$\Phi^j_{mq}\left(d_{j+1} + \Delta_j\right) = \delta_{mq} \exp\left(i\, r_q\, e_j\right). \tag{10.110}$$

10.5.4 Fields in the incident medium and substrate for conformal thin films

10.5.4.1 Incident field

The field amplitudes in Eq. (10.105) are defined in the transformed coordinate system. The amplitude of the incident field is given by Eq. (10.24), the field for the reflected **propagating** waves within the incident medium by Eq. (10.25), and the field for the transmitted **propagating** waves within the substrate by Eq. (10.26), in terms of the original Cartesian coordinate system. We now derive the form of these fields in the transformed coordinate system. The F component of the incident field is

$$F^i = \exp(i\, \alpha_0\, x) \exp\left(- i\, \beta_0^{Q+1}\, y\right) \tag{10.111}$$

$$= \exp(i\, \alpha_0\, v) \exp\left(- i\, \beta_0^{Q+1}\, u\right) \exp\left(- i\, \beta_0^{Q+1}\, a_{Q+1}(v)\right) \tag{10.112}$$

where we substitute for y using Eq. (10.29). The final exponential on the right hand side of Eq. (10.102) is periodic in v and can be expanded in a Fourier series. Substituting the generic t for β_0^{Q+1},

$$\exp\left(- i\, t\, a_{Q+1}(v)\right) = \sum_m L_m^{Q+1}(t) \exp(i\, m\, K\, v) \tag{10.113}$$

where

$$L_m^{Q+1}(t) =$$

$$\begin{cases} 1 & \text{if } a \text{ or } t = 0, \text{ and } m = 0 \\ 0 & \text{if } a \text{ or } t = 0, \text{ and } m \neq 0 \\ \frac{1}{d}\int_0^d \exp\left(-i\,t\,a_{Q+1}(v)\right)\cdot\exp\left(-i\,m\,K\,v\right)dv & \text{otherwise} \end{cases}.$$

We note that this is the same function as that given in Eq. (10.14) except that $a_{Q+1}(v)$ is substituted for Δ_{lj}. The integral in Eq. (10.114) becomes a summation over the line segments in the groove profile. Using Eq. (10.113) in Eq. (10.112) gives

$$F^i = \sum_m L_m^{Q+1}\left(\beta_0^{Q+1}\right)\exp\left(i\,\alpha_m\,v - i\,\beta_0^{Q+1}\,u\right) =$$

$$\begin{cases} \exp(i\,\alpha_0\,v) & \text{for } \beta_0^{Q+1} = 0 \\ \sum_m F_m^i\left(\beta_0^{Q+1}\right)\exp(i\,\alpha_m\,v) & \text{otherwise} \end{cases} \tag{10.115}$$

in the transformed coordinate system, where

$$F_m^i\left(\beta_0^{Q+1}\right) \equiv L_m^{Q+1}\left(\beta_0^{Q+1}\right)\exp\left(-i\,\beta_0^{Q+1}\,u\right). \tag{10.116}$$

The G component of the incident field is obtained from Eq. (10.55), remembering that the only nonzero component of F is F^3,

$$i\,\vec{\boldsymbol{G}}^i = \nabla\times\vec{\boldsymbol{F}}^i = \left(\frac{\partial F^{i3}}{\partial u}\right)\hat{\boldsymbol{e}}_1 - \left(\frac{\partial F^{i3}}{\partial v}\right)\hat{\boldsymbol{e}}_2 \tag{10.117}$$

or, remembering that G = G^1 and using Eqs. (10.38) and (10.43),

$$i\,G^i = \left[1 + \left(a'_{Q+1}\right)^2\right]\left(\frac{\partial F^{i3}}{\partial u}\right) - a'_{Q+1}\left(\frac{\partial F^{i3}}{\partial v}\right). \tag{10.118}$$

From Eq. (10.123),

$$\frac{\partial F^i}{\partial u} = -i\,\beta_0^{Q+1}\left[\exp(i\,\alpha_0\,v)\exp\left(-i\,\beta_0^{Q+1}\,u\right)\exp\left(-i\,\beta_0^{Q+1}\,a_{Q+1}(v)\right)\right] = -i\,\beta_0^{Q+1}\,F^i \tag{10.119}$$

and

$$\frac{\partial F^i}{\partial v} = i\,\alpha_0\left[\exp(i\,\alpha_0\,v)\exp\left(-i\,\beta_0^{Q+1}\,u\right)\exp\left(-i\,\beta_0^{Q+1}\,a_{Q+1}(v)\right)\right] - i\,\beta_0^{Q+1}\,a'_{Q+1}(v)\left[\exp(i\,\alpha_0\,v)\exp\left(-i\,\beta_0^{Q+1}\,u\right)\exp\left(-i\,\beta_0^{Q+1}\,a_{Q+1}(v)\right)\right] \tag{10.120}$$

$$= \left[i\,\alpha_0 - i\,\beta_0^{Q+1}\,a'_{Q+1}(v)\right]F^i. \tag{10.121}$$

Plugging Eqs. (10.127) and (10.129) into (10.126) gives

$$G^i = -\left[\beta_0^{Q+1} + \alpha_0\,a'_{Q+1}(v)\right]F^i. \tag{10.122}$$

From Eq. (10.121),

$$\frac{\partial}{\partial v}\exp\left(-i\,t\,a_{Q+1}(v)\right) = \frac{\partial}{\partial v}\sum_m L_m(t)\exp(i\,m\,K\,v) \tag{10.123}$$

or

$$-i\,t\,a'_{Q+1}(v)\exp\left(-i\,t\,a_{Q+1}(v)\right) = \sum_m i\,m\,K\,L_m(t)\exp(i\,m\,K\,v). \tag{10.124}$$

so

$$a'_{Q+1}(v)\exp\left(-i\,t\,a_{Q+1}(v)\right)=\sum_m -\left(\frac{m\,K}{t}\right)L_m(t)\exp(i\,m\,K\,v). \tag{10.125}$$

From Eqs. (10.120) and (10.133),

$$a'_{Q+1}(v)\,F^i=\left[a'_{Q+1}(v)\exp\left(-i\,\beta_0^{Q+1}\,a_{Q+1}(v)\right)\right]\exp(i\,\alpha_0\,x)\exp\left(-i\,\beta_0^{Q+1}\,u\right) \tag{10.126}$$

$$=\ -\sum_m\left(\frac{m\,K}{\beta_0^{Q+1}}\right)L_m(t)\exp(i\,\alpha_m\,x)\exp\left(-i\,\beta_0^{Q+1}\,u\right) \tag{10.127}$$

so we can substitute the expansions (10.123) and (10.135) into (10.130), giving

$$G^i=-\sum_m L_m^{Q+1}\left(\beta_0^{Q+1}\right)\left[\beta_0^{Q+1}-\left(\frac{\alpha_0\,m\,K}{\beta_0^{Q+1}}\right)\right]\exp\left(i\,\alpha_m\,v-i\,\beta_0^{Q+1}\,u\right) \tag{10.128}$$

$$=\ \sum_m G_m^i\left(\beta_0^{Q+1}\right)\exp(i\,\alpha_m\,v) \tag{10.129}$$

where

$$G_m^i\left(\beta_0^{Q+1}\right)\equiv\sum_m L_m^{Q+1}\left(\beta_0^{Q+1}\right)\left[-\beta_0^{Q+1}+m\,K\left(\frac{\alpha_0}{\beta_0^{Q+1}}\right)\right]\exp\left(-i\,\beta_0^{Q+1}\,u\right). \tag{10.130}$$

The total incident field has now been expressed in Eqs. (10.115) and (10.130) as a Fourier expansion in the grating period. In vector form,

$$\vec{\zeta}^{\,i} = \begin{pmatrix} \vec{I}' \\ \vec{I}'' \end{pmatrix}$$

where the 2N+1 $\hat{F}$ components are taken from Eq. (10.116),

$$\zeta'_m = L_m^{Q+1}\left(-\beta_0^{Q+1}\right)\exp\left(-i\,\beta_0^{Q+1}\,u\right) \tag{10.132}$$

and the 2N+1 $\hat{G}$ components are taken from Eq. (10.130),

$$\zeta''_m = \eta_j\left[-\beta_0^{Q+1} + m\,K\left(\frac{\alpha_0}{\beta_0^{Q+1}}\right)\right] L_m^{Q+1}\left(-\beta_0^{Q+1}\right)\exp\left(-i\,\beta_0^{Q+1}\,u\right) \tag{10.133}$$

where the η_j factor comes from Eq. (10.96). When matching boundary conditions at the top surface of the grating (u = 0), we note that the factor $\exp\left(-i\,\beta_0^{Q+1}\,u\right)$ in Eqs. (10.132) and (10.133) is equal to 1.

10.5.4.2 Reflected propagating field

As previously stated, the reflected field consists of P_r upward **propagating** plane wave modes in the original Cartesian coordinate system. In the transformed coordinate system, from Eqs. (10.25) and (10.29),

$$F^r = \sum_{n\in U_r} B_n^r \exp(i\,\alpha_n\,v)\exp\left(i\,\beta_n^{Q+1}\,u\right)\exp\left[i\,\beta_n^{Q+1}\,a_{Q+1}(v)\right]. \tag{10.134}$$

Again, the final factor on the right hand side is periodic and can be expanded in a Fourier series using Eq. (10.113),

$$\exp\left(i\,\beta_n^{Q+1}\,a_{Q+1}(v)\right) = \sum_m L_m^{Q+1}\left(+\beta_n^{Q+1}\right)\exp(i\,m\,K\,v) \tag{10.135}$$

so

$$F^r = \sum_{n \in U_r} B_n^r \sum_m L_m^{Q+1}\left(+\beta_n^{Q+1}\right) \exp\left(i\,\alpha_{n+m}\,v + i\,\beta_n^{Q+1}\,u\right). \tag{10.136}$$

Letting $m \to m$ - n,

$$F^r = \sum_{n \in U_r} B_n^r \sum_m L_{m-n}^{Q+1}\left(+\beta_n^{Q+1}\right) \exp\left(i\,\alpha_m\,v + i\,\beta_n^{Q+1}\,u\right). \tag{10.137}$$

The $\hat{G}$ field components are also obtained from the analog to Eq. (10.122),

$$i\,G^r = \left[1 + \left(a'_{Q+1}\right)^2\right]\left(\frac{\partial F^{r3}}{\partial u}\right) - a'_{Q+1}\left(\frac{\partial F^{r3}}{\partial v}\right). \tag{10.138}$$

where

$$\frac{\partial F_n^r}{\partial u} = i\,\beta_n^{Q+1}\,F_n^r. \tag{10.139}$$

$$\frac{\partial F_n^r}{\partial v} = i\,\alpha_n\,F_n^r + i\,\beta_n^{Q+1}\,a'_{Q+1}(v)\,F_n^r. \tag{10.140}$$

so

$$G_n^r = \left(\beta_n^{Q+1} - \alpha_n\,a'_{Q+1}\right)F_n^r. \tag{10.141}$$

Taking the derivative of Eq. (10.143),

$$\left(\frac{1}{i\,\beta_n^{Q+1}}\right)\frac{\partial}{\partial v}\exp\left(i\,\beta_n^{Q+1}\,a_j(v)\right) =$$

$$\left(\frac{1}{i\,\beta_n^{Q+1}}\right)\frac{\partial}{\partial v}\sum_m L_m^{Q+1}\left(+\beta_n^{Q+1}\right)\exp(i\,m\,K\,v)$$

for $\beta_n^{Q+1} \neq 0$. So

$$a'_{Q+1}(v)\exp\left(i\,\beta_n^{Q+1}\,a_j(v)\right) = \sum_m\left(\frac{m\,K}{\beta_n^{Q+1}}\right)L_m^{Q+1}\left(+\beta_n^{Q+1}\right)\exp(i\,m\,K\,v). \tag{10.143}$$

Combining Eqs. (10.143) and (10.151), the periodic function $a'_{Q+1}(v)\,F^r$ has the expansion

$$a'_{Q+1}(v)\,F^r = \sum_{n\in U_r} B_n^r \exp(i\,\alpha_n\,v)\left[a'_{Q+1}(v)\exp\left(i\,\beta_n^{Q+1}\,a_{Q+1}(v)\right)\right]\exp\left(i\,\beta_n^{Q+1}\,u\right) \tag{10.144}$$

$$= \sum_{n\in U_r} B_n^r \sum_m\left(\frac{m\,K}{\beta_n^{Q+1}}\right)L_m^{Q+1}\left(+\beta_n^{Q+1}\right)\exp(i\,\alpha_{n+m}\,v)\exp\left(i\,\beta_n^{Q+1}\,u\right) \tag{10.145}$$

for $\beta_n^{Q+1} \neq 0$ and letting $m \to m - n$,

$$= \sum_{n\in U_r} B_n^r \sum_m\left(\frac{(m-n)\,K}{\beta_n^{Q+1}}\right)L_{m-n}^{Q+1}\left(+\beta_n^{Q+1}\right)\exp(i\,\alpha_m\,v)\exp\left(i\,\beta_n^{Q+1}\,u\right). \tag{10.146}$$

Inserting Eqs. (10.145) and (10.154) into Eq. (10.149) gives

$$G_n^r = B_n^r \sum_m\left[\beta_n^{Q+1} - (m-n)\,K\left(\frac{\alpha_n}{\beta_n^{Q+1}}\right)\right]L_{m-n}^{Q+1}\left(+\beta_n^{Q+1}\right)\exp\left(i\,\alpha_m\,v + i\,\beta_n^{Q+1}\,u\right) \tag{10.147}$$

for $\beta_n^{Q+1} \neq 0$. It is entirely possible that a diffracted order will have a reflected angle of 0° for which $\beta_n^{Q+1} = 0$. Because we expect the field amplitude to change continuously as the diffracted angle scans through 0°, we can determine the value for G_n^r at $\beta_n^{Q+1} = 0$ by taking the limit,

$$G_n^r\left(\beta_n^{Q+1} = 0\right) = \lim_{\beta_n^{Q+1} \to 0} \Bigg(B_n^r \sum_m \left[\beta_n^{Q+1} - (m-n)\, K\left(\frac{\alpha_n}{\beta_n^{Q+1}}\right)\right] L_{m-n}^{Q+1}\left(+\beta_n^{Q+1}\right) \exp\left(i\, \alpha_m\, v + i\, \beta_n^{Q+1}\, u\right) \Bigg) \tag{10.148}$$

$$= \lim_{\beta_n^{Q+1} \to 0} \left(-B_n^r \sum_m \left[(m-n)\, K\left(\frac{\alpha_n}{\beta_n^{Q+1}}\right)\right] L_{m-n}^{Q+1}\left(+\beta_n^{Q+1}\right) \exp(i\, \alpha_m\, v) \right) \tag{10.149}$$

But for $m \neq 0$,

$$\lim_{t \to 0} L_m^{Q+1}(t) = \frac{1}{d} \int_0^d \left(1 - i\, t\, a_{Q+1}(v)\right) \cdot \exp(-i\, m\, K\, v)\, dv \tag{10.150}$$

$$= -\frac{i\, t}{d} \int_0^d a_{Q+1}(v) \cdot \exp(-i\, m\, K\, v)\, dv \tag{10.151}$$

so Eq. (10.149) becomes

$$G_n^r\left(\beta_n^{Q+1} = 0\right) = B_n^r \sum_m [(m-n)\, K\, \alpha_n] \left(\int_0^d \frac{i\, a_{Q+1}(v)}{d} \cdot \exp(-i\, (m-n)\, K\, v)\, dv \right) \exp(i\, \alpha_m\, v) \tag{10.152}$$

for $\beta_n^{Q+1} = 0$. Of course, the integral becomes a summation of integrals for our piecewise continuous groove profile. From Eq. (10.4),

$$\int_0^d a_{Q+1}(v) \cdot \exp(-i\, (m-n)\, K\, v)\, dv = \sum_{l=1}^{L} \int_{v_{l-1}}^{v_l} \left(a'_{l,Q+1}\, v + b_{l,Q+1}\right) \exp(-i\, (m-n)\, K\, v)\, dv \tag{10.153}$$

where

$$b_{l,Q+1} \equiv y_{l-1}^{Q+1} - \frac{\nu_{l-1}^{Q+1}\left(y_l^{Q+1} - y_{l-1}^{Q+1}\right)}{\nu_l^{Q+1} - \nu_{l-1}^{Q+1}}. \tag{10.154}$$

The total reflected propagating field can now be represented by a matrix equation,

$$\vec{\tilde{\zeta}}^{r} = \tilde{\boldsymbol{M}}' \vec{\boldsymbol{B}}^{r} \tag{10.155}$$

where $\vec{\tilde{\zeta}}^{r}$ is a 4N+2 component field vector, $\tilde{\boldsymbol{M}}'$ is a matrix with 4N+2 rows and P_r columns, and $\vec{\boldsymbol{B}}^{r}$ is a vector with P_r components of the unknown amplitudes of the reflected propagating plane waves. $\tilde{\boldsymbol{M}}'$ can be split into upper and lower matrices,

$$\tilde{\boldsymbol{M}}' \equiv \begin{pmatrix} \tilde{\boldsymbol{M}}'' \\ \tilde{\boldsymbol{M}}''' \end{pmatrix} \tag{10.156}$$

where according to Eqs. (10.137) and (10.147),

$$M''_{mn} = \begin{cases} L_{m-n}^{Q+1}\left(+\beta_n^{Q+1}\right) \exp\left(i\,\beta_n^{Q+1}\,u\right) & \text{for } \beta_n^{Q+1} \neq 0 \\ 0 & \text{for } \beta_n^{Q+1} = 0 \end{cases} \tag{10.157}$$

and

$$M'''_{mn} = \begin{cases} \eta_j\left[\beta_n^{Q+1} - (m-n)\,K\left(\frac{\alpha_n}{\beta_n^{Q+1}}\right)\right] L_{m-n}^{Q+1}\left(+\beta_n^{Q+1}\right) \exp\left(i\,\beta_n^{Q+1}\,u\right) & \text{for } \beta_n^{Q+1} \neq 0 \\ \eta_j[(m-n)\,K\,\alpha_n]\left(\int_0^d \frac{i\,a_{Q+1}(v)}{d} \cdot \exp(-i\,(m-n)\,K\,v)\,dv\right) & \text{for } \beta_n^{Q+1} = 0 \end{cases} \tag{10.158}$$

.

In Eqs. (10.157) and (10.158), the m index runs between -N and +N while the n index corresponds to the P_r modes that are propagating in the upward direction, i.e., for which

$$\text{Im}\left(\beta_n^{Q+1}\right) = 0 \qquad \text{and} \qquad \text{Re}\left(\beta_n^{Q+1}\right) > 0. \tag{10.159}$$

Once again, at the top surface the factor $\exp\left(i\,\beta_n^{Q+1}\,u\right)$ is equal to 1.

10.5.4.3 Reflected evanescent field

There are only P_r reflected propagating modes given by Eq. (10.155), but there are a total of 2N+1 modes with $\mathrm{Re}\left(\beta_n^{Q+1}\right) > 0$ in the upper dielectric medium. The remaining $2N+1-P_r$ modes which are not propagating modes must be evanescent modes. The evanescent modes can be represented by the eigenvectors from Eq. (10.101),

$$\vec{\zeta}^{er} = \sum_{q\notin U} b_q^{Q+1}\,\tilde{\mathbf{V}}_q^{Q+1}\exp\left(i\,r_q^j\,u\right) \tag{10.160}$$

such that

$$\mathrm{Im}\left(r_q^{Q+1}\right) > 0. \tag{10.161}$$

In terms of the M matrix,

$$\vec{\zeta}^{er} = \tilde{\mathrm{M}}^{Q+1}\,\tilde{\mathbf{\Phi}}^{Q+1}\left(u_{Q+1}\right)\vec{\boldsymbol{b}}^{Q+1} \tag{10.162}$$

where the $\hat{\boldsymbol{M}}^{Q+1}$ matrix in this case is a rectangular matrix with 4N+2 rows and only those $2N+1-P_r$ columns for which the eigenvector corresponds to one of the eigenval ues satisfying inequality (10.161). The total field in the incident medium is thus

$$\vec{\zeta}^{R} = \vec{\zeta}^{i} + \vec{\zeta}^{r} + \vec{\zeta}^{er} \tag{10.163}$$

in which there are 2N+1 total unknown amplitudes.

Transmitted propagating field

By Eqs. (10.26) and (10.29) the transmitted **propagating** modes are given by the expansion

$$F^t = \sum_{n\in U_t} B_n^t\exp\left(i\,\alpha_n\,v - i\,\beta_n^0(u+a_1(v))\right). \tag{10.164}$$

$$\exp\left(-i\,\beta_n^0\,a_1(v)\right) = \sum_m L_m^1\left(-\beta_n^0\right)\exp(i\,m\,K\,v) \tag{10.165}$$

$$F^t = \sum_{n \in U_t} B_n^t \exp(i\,\alpha_n\,v) \exp\left(-i\,\beta_n^0\,u\right) \exp\left(-i\,\beta_n^0\,a_1(v)\right) \tag{10.166}$$

$$= \sum_{n \in U_t} B_n^t \exp\left(-i\,\beta_n^0\,u\right) \sum_m L_m^1\left(-\beta_n^0\right) \exp(i\,\alpha_{n+m}\,v) \tag{10.167}$$

$$= \sum_{n \in U_t} B_n^t \sum_m L_{m-n}^1\left(-\beta_n^0\right) \exp\left(i\,\alpha_m\,v - i\,\beta_n^0\,u\right). \tag{10.168}$$

The $\hat{G}$ field components are once again obtained from the analog to Eq. (10.122),

$$i\,G^t = \left[1 + \left(a_0'\right)^2\right]\left(\frac{\partial F^{t3}}{\partial u}\right) - a_0'\left(\frac{\partial F^{t3}}{\partial v}\right) \tag{10.169}$$

where

$$\frac{\partial F_n^t}{\partial u} = -i\,\beta_n^0\,F_n^t. \tag{10.170}$$

$$\frac{\partial F_n^t}{\partial v} = i\,\alpha_n\,F_n^t - i\,\beta_n^0\,a_0'(v)\,F_n^t. \tag{10.171}$$

so

$$G_n^t = -\left[\,\beta_n^0 + \alpha_n\,a_0'(v)\right]F_n^t. \tag{10.172}$$

From Eq. (10.165),

$$\frac{\partial}{\partial v}\exp\left(-\,i\,\beta_n^0\,a_1(v)\right) = \frac{\partial}{\partial v}\sum_m L_m^1\left(-\beta_n^0\right)\exp(i\,m\,K\,v) \tag{10.173}$$

$$a_1'(v)\exp\left(-i\,\beta_n^0\,a_1(v)\right) = -\sum_m \frac{m\,K}{\beta_n^0}\,L_m^1\left(-\beta_n^0\right)\exp(i\,m\,K\,v) \tag{10.174}$$

and

$$a_1'(v)\,F^t = \sum_{n\in U_t} B_n^t \exp(i\,\alpha_n\,v)\left[a_1'(v)\exp\left(-i\,\beta_n^0\,u\right)\right]\exp\left(-i\,\beta_n^0\,a_1(v)\right) \tag{10.175}$$

$$= -\sum_{n\in U_t} B_n^t \sum_m \frac{m\,K}{\beta_n^0}\,L_m^1\left(-\beta_n^0\right)\exp(i\,\alpha_{n+m}\,v)\exp\left(-i\,\beta_n^0\,a_1(v)\right) \tag{10.176}$$

$$= -\sum_{n\in U_t} B_n^t \sum_m \frac{(m-n)\,K}{\beta_n^0}\,L_{m-n}^1\left(-\beta_n^0\right)\exp(i\,\alpha_m\,v)\exp\left(-i\,\beta_n^0\,a_1(v)\right) \tag{10.177}$$

Then substituting Eqs. (10.168) and (10.177) into Eq. (10.172) gives

$$G_n^t = \sum_m\left[-\beta_n^0 + (m-n)\,K\,\frac{\alpha_n}{\beta_n^0}\right]L_{m-n}^1\left(-\beta_n^0\right)\exp\left(i\,\alpha_m\,v - i\,\beta_n^0\,u\right)B_n^t. \tag{10.178}$$

The P_t transmitted propagating modes are represented by the matrix equation

$$\vec{\boldsymbol{\zeta}}^t = \tilde{\boldsymbol{N}}'\,\vec{\boldsymbol{B}}^t \tag{10.179}$$

where $\vec{\boldsymbol{\zeta}}^t$ is a 4N+2 component transmitted field vector, $\vec{\boldsymbol{B}}^t$ is a vector of the P_t unknown transmitted field amplitudes, and $\tilde{\boldsymbol{N}}'$ is a rectangular matrix with 4N+2 rows and P_t columns which can be divided into an upper and lower matrix, each with 2N+1 rows,

$$\tilde{\boldsymbol{N}}' = \begin{pmatrix} \tilde{\boldsymbol{N}}'' \\ \tilde{\boldsymbol{N}}''' \end{pmatrix}, \tag{10.180}$$

defined according to Eqs. (10.168) and (10.178),

$$N_{mn}'' = L_{m-n}^1\left(-\beta_n^0\right)\exp\left(-i\,\beta_n^0\,u\right) \tag{10.181}$$

and

$$N'''_{mn} = \eta_j \left[-\beta_n^0 + (m-n)\, K\, \frac{\alpha_n}{\beta_n^0} \right] L^1_{m-n}\left(-\beta_n^0\right)\, \exp\left(-i\, \beta_n^0\, u\right). \tag{10.182}$$

As with the corresponding equation for the reflected field, the *m* index in these matrices ranges from -N to +N, while the *n* index covers all P_t values for which

$$\mathrm{Im}\left(\beta_n^0\right) = 0 \qquad \text{and} \qquad \mathrm{Re}\left(\beta_n^0\right) < 0. \tag{10.183}$$

At the bottom surface of the grating, the factor $\exp\left(-i\, \beta_n^0\, u\right)$ in Eqs. (10.181) and (10.182) is equal to 1.

10.5.4.4 Transmitted evanescent field

Finally, there are $2N + 1 - P_t$ evanescent modes in the substrate and we can use the previously derived field expression in the transformed coordinate system, Eq. (10.105), to express these components,

$$\vec{\zeta}^{et} = \tilde{\mathrm{M}}_{ev}^0\, \vec{\boldsymbol{b}}_{ev}^0, \tag{10.184}$$

where $\vec{\zeta}^{et}$ is the evanescent field vector in the substrate with 4N+2 components, $\tilde{\mathrm{M}}_{ev}^0$ is a rectangular matrix with 4N+2 rows and $2N + 1 - P_t$ columns, and $\vec{\boldsymbol{b}}_{ev}^0$ is a vector with $2N + 1 - P_t$ unknown evanescent field amplitudes. The columns in $\tilde{\mathrm{M}}_{ev}^0$ correspond to the columns in $\tilde{\mathrm{M}}^0$ which represent these evanescent modes, i.e., for which the eigenvalues satisfy the condition

$$\mathrm{Im}\left(r_q^0\right) < 0. \tag{10.185}$$

The total transmitted field is then

$$\vec{\boldsymbol{\zeta}}^T = \vec{\boldsymbol{\zeta}}^t + \vec{\boldsymbol{\zeta}}^{et} = \tilde{\boldsymbol{N}}'\, \vec{\boldsymbol{B}}^t + \tilde{\mathrm{M}}_{ev}^0\, \vec{\boldsymbol{b}}_{ev}^0 \equiv \tilde{\mathrm{M}}_s \begin{pmatrix} \vec{\boldsymbol{B}}^t \\ \vec{\boldsymbol{b}}_{ev}^0 \end{pmatrix} \tag{10.186}$$

where we have defined the new square matrix $\tilde{\mathrm{M}}_s$ with rank 2N+1 that is obtained by combining $\tilde{\boldsymbol{N}}'$ and $\tilde{\mathrm{M}}_{ev}^0$.

10.5.5 Boundary conditions for conformal thin films

The unknown field amplitudes in $\hat{F}$ and $\hat{G}$ within each layer are determined by satisfying the boundary conditions. We know that the tangential components of the $\vec{\boldsymbol{E}}$ and $\vec{\boldsymbol{H}}$ fields are continuous across each interface. We now start with the simplest case, that for which all layers have the identical groove profile. For **TE polarization**, the E field lies along the w (z) axis and is tangential to each interface. The H field is orthogonal to the E field and H^1 is the component of the H field which is tangential to the interface, because it is parallel to the $\hat{\boldsymbol{e}}_1$ basis vector,

$$\vec{\boldsymbol{e}}_1 \cdot \vec{\boldsymbol{H}} = H^1. \tag{10.187}$$

By Eq. (10.53),

$$\hat{F} \equiv F = E_w \tag{10.188}$$

and

$$\hat{G}_m = \eta_j G_m^1 = \frac{G_m^1}{\mu_r} = \frac{\gamma_1 H^1}{\mu_r} = k_0 Z_0 H^1. \tag{10.189}$$

Therefore, $\hat{F}$ and $\hat{G}$ as defined in Eqs. (10.95) and (10.96) are proportional to E_w and H^1, respectively, and must also be continuous across each interface for TE polarization.

For **TM polarization**, the $\vec{\boldsymbol{H}}$ field is along the w (z)-direction and is tangential to each interface. The E^1 field component is orthogonal to the $\vec{\boldsymbol{H}}$ field and is tangential to the interface. Using Eq. (10.54) and the following definitions for $\hat{F}$ and $\hat{G}$,

$$\hat{F} \equiv F = Z_0 H_w \tag{10.190}$$

and

$$\hat{G} = \eta_j G_m^1 = \frac{-Z_0 \gamma_2 E^1}{\epsilon_r} = -k_0 E^1, \tag{10.191}$$

we find that $\hat{F}$ and $\hat{G}$ are again both proportional to field components that are continuous across each interface. Therefore, **for the conformal multilayer film stack, the vector $\vec{\hat{\zeta}}$ defined in Eq. (10.97) is continuous across each interface for both TE and TM polarizations**.

The boundary condition at the top of layer j is

$$\vec{\hat{\zeta}}^{\,j+1}\left(u = d_{j+1}\right) = \vec{\hat{\zeta}}^{\,j}\left(u = d_{j+1}\right) \tag{10.192}$$

By Eq. (10.105), and remembering that the phase factor is defined to be zero at the bottom interface of a given layer,

$$\tilde{\mathrm{M}}^{j+1}\,\tilde{\boldsymbol{\Phi}}^{j+1}\left(d_{j+1}\right)\vec{\boldsymbol{b}}^{j+1} = \tilde{\mathrm{M}}^{j+1}\,\vec{\boldsymbol{b}}^{j+1} = \tilde{\mathrm{M}}^{j}\,\tilde{\boldsymbol{\Phi}}^{j}\left(d_{j+1}\right)\vec{\boldsymbol{b}}^{j}. \tag{10.193}$$

10.5.6 Transfer matrix for conformal thin films

Eq. (10.193) provides the basic mechanism for generating the transfer matrix that connects the fields at the top surface of the films to the fields within the substrate. For multiple thin film layers,

$$\tilde{\mathrm{M}}^{Q+1}\,\vec{\boldsymbol{b}}^{Q+1} = \tilde{\mathrm{M}}^{Q}\,\tilde{\boldsymbol{\Phi}}^{Q}\left(d_{Q+1}\right)\vec{\boldsymbol{b}}^{Q} = \tilde{\mathrm{M}}^{Q}\,\tilde{\boldsymbol{\Phi}}^{Q}\left(d_{Q+1}\right)\left(\tilde{\mathrm{M}}^{Q}\right)^{-1}\tilde{\mathrm{M}}^{Q-1}\,\tilde{\boldsymbol{\Phi}}^{Q-1}\left(d_{Q}\right)\vec{\boldsymbol{b}}^{Q-1} \tag{10.194}$$

$$= \left[\tilde{\mathrm{M}}^{Q}\,\tilde{\boldsymbol{\Phi}}^{Q}\left(\tilde{\mathrm{M}}^{Q}\right)^{-1}\right]\left[\tilde{\mathrm{M}}^{Q-1}\,\tilde{\boldsymbol{\Phi}}^{Q-1}\left(\tilde{\mathrm{M}}^{Q-1}\right)^{-1}\right]\cdots\left[\tilde{\mathrm{M}}^{1}\,\tilde{\boldsymbol{\Phi}}^{1}\left(\tilde{\mathrm{M}}^{1}\right)^{-1}\right]\tilde{\mathrm{M}}^{0}\,\tilde{\boldsymbol{\Phi}}^{0}\,\vec{\boldsymbol{b}}^{0} \tag{10.195}$$

$$= \left[\tilde{\boldsymbol{H}}^{Q}\,\tilde{\boldsymbol{H}}^{Q-1}\cdots\tilde{\boldsymbol{H}}^{1}\right]\tilde{\mathrm{M}}^{0}\,\tilde{\boldsymbol{\Phi}}^{0}\left(d_{0}\right)\vec{\boldsymbol{b}}^{0} = \tilde{\boldsymbol{H}}\left(\tilde{\mathrm{M}}^{0}\,\vec{\boldsymbol{b}}^{0}\right) \tag{10.196}$$

where

$$\tilde{\boldsymbol{H}}^{j} \equiv \tilde{\mathrm{M}}^{j}\left[\tilde{\boldsymbol{\Phi}}^{j}\left(d_{j+1}\right)\right]\left(\tilde{\mathrm{M}}^{j}\right)^{-1} \tag{10.197}$$

and

$$\tilde{\boldsymbol{H}} \equiv \tilde{\boldsymbol{H}}^{Q}\,\tilde{\boldsymbol{H}}^{Q-1}\cdots\tilde{\boldsymbol{H}}^{1}. \tag{10.198}$$

$\tilde{\boldsymbol{H}}$ is the transfer matrix, a square matrix of rank 4N+2. Eqs. (10.194)-(10.196) connect the unknown field amplitudes inside the substrate, $\vec{\boldsymbol{b}}^{0}$, to the unknown field amplitudes in the incident medium, $\vec{\boldsymbol{b}}^{Q+1}$, via the transfer matrix $\tilde{\boldsymbol{H}}$.

$\tilde{\mathrm{M}}^{Q+1}\vec{\boldsymbol{b}}^{Q+1}$ in Eq. (10.194) is the total field in the incident medium at the top surface, which was derived in Eq. (10.163). $\tilde{\mathrm{M}}^{0}\vec{\boldsymbol{b}}^{0}$ is the total transmitted field at the bottom interface, which was derived in Eq. (10.186). Therefore, we can rewrite Eqs. (10.194)-(10.196) as

$$\vec{\boldsymbol{\zeta}}^{R}\left(u_{Q+1}\right) = \tilde{\boldsymbol{H}}\,\vec{\boldsymbol{\zeta}}^{T}\left(u_{0}\right). \tag{10.199}$$

This matrix equation may be separated into 4N+2 linear equations with 4N+2 unknown amplitudes, and thus it provides the solution for all the unknown b^{0} and b^{Q+1} amplitudes. Once these amplitudes are known, the amplitudes for the field within any other layer are found simply by truncating Eq. (10.194) at the appropriate layer.

It may not be imediately obvious, however, how to solve Eq. (10.199). The procedure is as follows. First we expand Eq. (10.199) into all of its components.

$$\begin{aligned} &\vec{\hat{\boldsymbol{\zeta}}}^{i} + \boldsymbol{M}'\,\vec{\boldsymbol{B}}^{r} + \tilde{\mathrm{M}}^{Q+1}\,\tilde{\boldsymbol{\Phi}}^{Q+1}\left(u_{Q+1}\right)\vec{\boldsymbol{b}}^{Q+1} = \\ &\tilde{\boldsymbol{H}}\left(\tilde{\boldsymbol{N}}'\,\vec{\boldsymbol{B}}^{t} + \tilde{\mathrm{M}}^{0}\,\vec{\boldsymbol{b}}^{0}\right) = \left(\tilde{\boldsymbol{H}}\,\tilde{\boldsymbol{N}}'\right)\vec{\boldsymbol{B}}^{t} + \left(\tilde{\boldsymbol{H}}\,\tilde{\mathrm{M}}^{0}\right)\vec{\boldsymbol{b}}^{0}. \end{aligned} \tag{10.200}$$

Solving for $\vec{\hat{\boldsymbol{\zeta}}}^{i}$ and remembering that the definition of the phase factor means that $\tilde{\boldsymbol{\Phi}}^{Q+1}$ is the identity matrix,

$$-\boldsymbol{M}'\,\vec{\boldsymbol{B}}^{r} - \tilde{\mathrm{M}}^{Q+1}\,\vec{\boldsymbol{b}}^{Q+1} + \left(\tilde{\boldsymbol{H}}\,\tilde{\boldsymbol{N}}'\right)\vec{\boldsymbol{B}}^{t} + \left(\tilde{\boldsymbol{H}}\,\tilde{\mathrm{M}}^{0}\right)\vec{\boldsymbol{b}}^{0} = \vec{\hat{\boldsymbol{\zeta}}}^{i}. \tag{10.201}$$

Now, the matrices on the left hand side of this equation all have 4N+2 rows, and the total number of columns is also 4N+2, so they can be combined into a single square matrix, $\tilde{\boldsymbol{Z}}$, with rank 4N+2,

$$\tilde{\boldsymbol{Z}} = \left[\, -\boldsymbol{M}' \qquad -\tilde{\mathrm{M}}^{\boldsymbol{Q+1}} \qquad \tilde{\boldsymbol{H}}\,\tilde{\boldsymbol{N}}' \qquad \tilde{\boldsymbol{H}}\,\tilde{\mathrm{M}}^{0}\,\right]. \tag{10.202}$$

We also define the new vector of the 4N+2 unknown amplitudes,

$$\vec{\boldsymbol{B}} = \begin{pmatrix} \vec{\boldsymbol{B}}^{r} \\ \vec{\boldsymbol{b}}^{Q+1} \\ \vec{\boldsymbol{B}}^{t} \\ \vec{\boldsymbol{b}}^{0} \end{pmatrix}. \tag{10.203}$$

Then

$$\tilde{\boldsymbol{Z}}\, \vec{\boldsymbol{B}} = \vec{\hat{\boldsymbol{\zeta}}}^{i} \tag{10.204}$$

or

$$\vec{\boldsymbol{B}} = (\tilde{\boldsymbol{Z}})^{-1}\, \vec{\hat{\boldsymbol{\zeta}}}^{i}. \tag{10.205}$$

The quantities on the right hand side of this equation are all known or can be computed from the groove profile and the optical properties of the thin film stack. The vector on the left hand side includes all the unknown field amplitudes within the incident medium and the substrate.

A simple example makes this much more obvious. Let us consider the case where N = 1, and P_r and P_t are both equal 1 as well. Thus, there will be two evanescent modes (2N+1-P) in both incident and transmitted media. Let $\tilde{\mathrm{M}}^{0}$ be so arranged that the column vectors in $\tilde{\mathrm{M}}^{0}$ corresponding to the evanescent modes satisfying inequality (10.185) are the last two columns of this 6 × 6 matrix, and let $\tilde{\mathrm{M}}^{Q+1}$ be arranged so that the column vectors satisfying inequality (10.161) are the second and third columns. Then Eq. (10.199) can be written

$$\begin{pmatrix} F_{-1}^{i} \\ F_{0}^{i} \\ F_{+1}^{i} \\ G_{-1}^{i} \\ G_{0}^{i} \\ G_{+1}^{i} \end{pmatrix} + \begin{pmatrix} M_{11}'' \\ M_{21}'' \\ M_{31}'' \\ M_{41}'''' \\ M_{51}'''' \\ M_{61}'''' \end{pmatrix} b_1^r + \begin{pmatrix} M_{15}^{Q+1} & M_{16}^{Q+1} \\ M_{25}^{Q+1} & M_{26}^{Q+1} \\ M_{35}^{Q+1} & M_{36}^{Q+1} \\ M_{45}^{Q+1} & M_{46}^{Q+1} \\ M_{55}^{Q+1} & M_{56}^{Q+1} \\ M_{65}^{Q+1} & M_{66}^{Q+1} \end{pmatrix} \begin{pmatrix} b_5^{Q+1} \\ b_6^{Q+1} \end{pmatrix} =$$

$$\begin{pmatrix} H_{11} & H_{12} & H_{13} & H_{14} & H_{15} & H_{16} \\ H_{21} & H_{22} & H_{23} & H_{24} & H_{25} & H_{26} \\ H_{31} & H_{32} & H_{33} & H_{34} & H_{35} & H_{36} \\ H_{41} & H_{42} & H_{43} & H_{44} & H_{45} & H_{46} \\ H_{51} & H_{52} & H_{53} & H_{54} & H_{55} & H_{56} \\ H_{61} & H_{62} & H_{64} & H_{64} & H_{65} & H_{61} \end{pmatrix} \left(\begin{pmatrix} N_{11}'' \\ N_{21}'' \\ N_{31}'' \\ N_{41}'''' \\ N_{51}'''' \\ N_{61}'''' \end{pmatrix} b_1^t + \begin{pmatrix} M_{12}^0 + M_{13}^0 \\ M_{22}^0 + M_{23}^0 \\ M_{32}^0 + M_{33}^0 \\ M_{42}^0 + M_{43}^0 \\ M_{52}^0 + M_{53}^0 \\ M_{62}^0 + M_{64}^0 \end{pmatrix} \begin{pmatrix} b_2^0 \\ b_3^0 \end{pmatrix} \right)$$

$$\begin{pmatrix} F_{-1}^{i} \\ F_{0}^{i} \\ F_{+1}^{i} \\ G_{-1}^{i} \\ G_{0}^{i} \\ G_{+1}^{i} \end{pmatrix} + \begin{pmatrix} M_{11}'' & M_{15}^{Q+1} & M_{16}^{Q+1} \\ M_{21}'' & M_{25}^{Q+1} & M_{26}^{Q+1} \\ M_{31}'' & M_{35}^{Q+1} & M_{36}^{Q+1} \\ M_{41}'''' & M_{45}^{Q+1} & M_{46}^{Q+1} \\ M_{51}'''' & M_{55}^{Q+1} & M_{56}^{Q+1} \\ M_{61}'''' & M_{65}^{Q+1} & M_{66}^{Q+1} \end{pmatrix} \begin{pmatrix} b_1^r \\ b_5^{Q+1} \\ b_6^{Q+1} \end{pmatrix} = \begin{pmatrix} H_{11}' & H_{12}' & H_{13}' \\ H_{21}' & H_{22}' & H_{23}' \\ H_{31}' & H_{32}' & H_{33}' \\ H_{41}' & H_{42}' & H_{43}' \\ H_{51}' & H_{52}' & H_{53}' \\ H_{61}' & H_{62}' & H_{64}' \end{pmatrix} \begin{pmatrix} b_1^t \\ b_2^0 \\ b_3^0 \end{pmatrix} \tag{10.207}$$

where the $\tilde{\boldsymbol{H}}$ matrix multiplication has been performed to obtain the new matrix $\tilde{\boldsymbol{H}}'$ and the right hand side of the equation has been simplified into a single matrix product. Then the matrices can be rearranged and combined,

$$\begin{pmatrix} -M''_{11} & -M_{15}^{Q+1} & -M_{16}^{Q+1} & H'_{11} & H'_{12} & H'_{13} \\ -M''_{21} & -M_{25}^{Q+1} & -M_{26}^{Q+1} & H'_{21} & H'_{22} & H'_{23} \\ -M''_{31} & -M_{35}^{Q+1} & -M_{36}^{Q+1} & H'_{31} & H'_{32} & H'_{33} \\ -M'''_{41} & -M_{45}^{Q+1} & -M_{46}^{Q+1} & H'_{41} & H'_{42} & H'_{43} \\ -M'''_{51} & -M_{55}^{Q+1} & -M_{56}^{Q+1} & H'_{51} & H'_{52} & H'_{53} \\ -M'''_{61} & -M_{65}^{Q+1} & -M_{66}^{Q+1} & H'_{61} & H'_{62} & H'_{64} \end{pmatrix} \begin{pmatrix} b_1^r \\ b_5^{Q+1} \\ b_6^{Q+1} \\ b_1^t \\ b_2^0 \\ b_3^0 \end{pmatrix} = \begin{pmatrix} F_{-1}^i \\ F_0^i \\ F_{+1}^i \\ G_{-1}^i \\ G_0^i \\ G_{+1}^i \end{pmatrix}. \tag{10.208}$$

or

$$\begin{pmatrix} b_1^r \\ b_5^{Q+1} \\ b_6^{Q+1} \\ b_1^t \\ b_2^0 \\ b_3^0 \end{pmatrix} = \begin{pmatrix} -M''_{11} & -M_{15}^{Q+1} & -M_{16}^{Q+1} & H'_{11} & H'_{12} & H'_{13} \\ -M''_{21} & -M_{25}^{Q+1} & -M_{26}^{Q+1} & H'_{21} & H'_{22} & H'_{23} \\ -M''_{31} & -M_{35}^{Q+1} & -M_{36}^{Q+1} & H'_{31} & H'_{32} & H'_{33} \\ -M'''_{41} & -M_{45}^{Q+1} & -M_{46}^{Q+1} & H'_{41} & H'_{42} & H'_{43} \\ -M'''_{51} & -M_{55}^{Q+1} & -M_{56}^{Q+1} & H'_{51} & H'_{52} & H'_{53} \\ -M'''_{61} & -M_{65}^{Q+1} & -M_{66}^{Q+1} & H'_{61} & H'_{62} & H'_{64} \end{pmatrix}^{-1} \begin{pmatrix} F_{-1}^i \\ F_0^i \\ F_{+1}^i \\ G_{-1}^i \\ G_0^i \\ G_{+1}^i \end{pmatrix}. \tag{10.209}$$

10.5.7 Boundary conditions for nonconformal thin films

If the groove profiles are not conformal, as shown in Fig. 10.32, then the situation is more complicated. The E_w and H_w field components along the w (z)-direction are continuous as before, so the boundary condition for $\hat{F}$ remains the same,

$$\hat{F}^{j+1}\left(u_{j+1} = d_{j+1}\right) = \hat{F}^{j}\left(u_j = d_{j+1} + \Delta_j(v)\right). \tag{10.210}$$

$\Delta_j(v)$ is a periodic function of v.

The G^1 field component in layer j is no longer tangential to the j+1 interface, so $\eta_j G^1$ is no longer continuous across the interface. G^1 and G_u in the j' th layer must be appropriately combined to obtain the field component that is tangential to the j+1 interface.

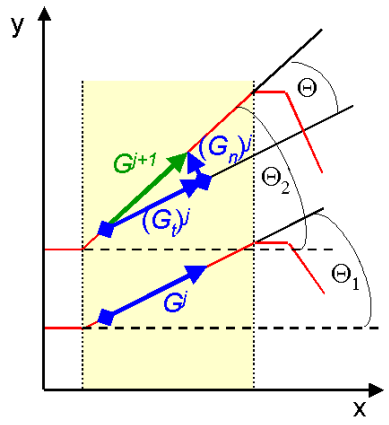

Fig. 10.32. The groove profile for two adjacent layers is shown in red. One segment of the profile is highlighted in yellow. The included angle between the groove profile of the two layers in this segment is Θ. Field G^j is the field component in layer *j* which is tangent to the bottom surface of layer *j*, and field $G^{j+1}$is the field component in layer *j+1* which is tangent to the bottom surface of layer *j+1*. G_u is the field component in layer *j* which is normal to the bottom surface of layer *j*.

Referring to Fig. 10.32, it is clear that the field component of *G* in the *j*'th layer which is tangential to the *j*+1 interface is

$$\hat{G}^j = \hat{G}_t^j \cos\Theta + \hat{G}_n^j \sin\Theta. \tag{10.211}$$

where

$$\hat{G}_t^j = \hat{\boldsymbol{e}}_1 \cdot \vec{\hat{\boldsymbol{G}}} = \frac{\vec{\boldsymbol{e}}_1}{\sqrt{1+\left(a'_j\right)^2}} \cdot \vec{\hat{\boldsymbol{G}}} = \frac{\hat{G}^{1,j}}{\sqrt{1+\left(a'_j\right)^2}} \tag{10.212}$$

and

$$\hat{G}_n^j = \hat{\boldsymbol{e}}^2 \cdot \vec{\hat{\boldsymbol{G}}} = \frac{\vec{\boldsymbol{e}}^2}{\sqrt{1+\left(a'_j\right)^2}} \cdot \vec{\hat{\boldsymbol{G}}} = \frac{\hat{G}_u^j}{\sqrt{1+\left(a'_j\right)^2}}. \tag{10.213}$$

Θ is the angle between the line segment of the *j*+1 interface and the *j* interface, which can be written in terms of the slopes of these line segments as follows.

$$\Theta = \Theta_2 - \Theta_1 \tag{10.214}$$

where

$$\tan\Theta_2 = a'_{j+1} \quad \text{and} \quad \tan\Theta_1 = a_j{}' . \tag{10.215}$$

With a little algebraic manipulation and making use of standard trigonometric identities, one finds

$$\cos\Theta = \left(1 + a_j{}' \cdot a'_{j+1}\right) \Big/ \left(\sqrt{1 + \left(a'_j\right)^2}\ \sqrt{1 + \left(a'_{j+1}\right)^2}\right) \tag{10.216}$$

and

$$\sin\Theta = \left(a'_{j+1} - a'_j\right) \Big/ \left(\sqrt{1 + \left(a'_j\right)^2}\ \sqrt{\left(1 + \left(a'_{j+1}\right)^2\right)}\right). \tag{10.217}$$

Combining Eqs. (10.219) - (10.221), (10.224) and (10.225) gives

$$\hat{G}^j = \left(\left(1 + a'_j \cdot a'_{j+1}\right)\hat{G}^{1,j} + \left(a'_{j+1} - a'_j\right)\hat{G}_u^j\right) \Big/ \left(\left[1 + \left(a'_j\right)^2\right]\sqrt{\left(1 + \left(a'_{j+1}\right)^2\right)}\right). \tag{10.218}$$

This field is tangential to the j+1 interface and is, therefore, equal to the tangential component of the field in the j+1 medium,

$$\hat{G}_t^{j+1} = \frac{\hat{G}^{1,j+1}}{\sqrt{1 + \left(a'_{j+1}\right)^2}} = \left(\left(1 + a'_j \cdot a'_{j+1}\right)\hat{G}^{1,j} + \left(a'_{j+1} - a'_j\right)\hat{G}_u^j\right) \Big/ \left(\left[1 + \left(a'_j\right)^2\right]\sqrt{\left(1 + a'_{j+1}\right)^2}\right) \tag{10.219}$$

or

$$\hat{G}^{j+1} = \frac{\left(1 + a'_j \cdot a'_{j+1}\right)}{1 + \left(a'_j\right)^2} \hat{G}^j + \frac{\left(a'_{j+1} - a'_j\right)}{1 + \left(a'_j\right)^2} \hat{G}_u^j \tag{10.220}$$

where we have dropped the "1" superscript as was done previously following Eq. (10.66). This result can be further simplified by making use of the definitions in Eqs. (10.23) and (10.24) for C_j and D_j, as well as Eq. (10.15) for Δ'_j.

$$\Delta'_j D_j + 1 = \left(a'_{j+1} - a'_j\right)\left(\frac{a'_j}{1 + \left(a'_j\right)^2}\right) + 1 = \frac{1 + a'_j \cdot a'_{j+1}}{1 + \left(a'_j\right)^2} \tag{10.221}$$

and

$$\hat{G}^{j+1} = \left(\Delta'_j D_j + 1\right)\hat{G}^j + \Delta'_j C_j \hat{G}_u^j \tag{10.222}$$

within each of the n line segments of the groove profile. We now want to eliminate $\hat{G}_u$ from the boundary condition in Eq. (10.228) and express this equation in terms of the $\hat{G}$ and $\hat{F}$ fields only. From Eq. (10.63) we have

$$\vec{\boldsymbol{e}}^2 \cdot \left(\nabla \times \vec{\boldsymbol{F}}\right) = \vec{\boldsymbol{e}}^2 \cdot \boldsymbol{i}\, \vec{\boldsymbol{G}} \tag{10.223}$$

or

$$\frac{\partial F^1}{\partial w} - \frac{\partial F^3}{\partial v} = i\, G_u. \tag{10.224}$$

There is no field dependence along the w-direction, so the first term is zero. Indeed, F^3 is the only nonzero component of F, so we previously dropped the superscript "3." So we can replace G_u in Eq. (10.230) by a function of F from Eq. (10.232),

$$\hat{G}^{j+1} = \left(\Delta'_j(\nu)\, D_j + 1\right) \hat{G}^j + i\, \Delta'_j(\nu)\, \eta_j\, C_j\, \frac{\partial \hat{F}}{\partial \nu}. \tag{10.225}$$

$\Delta'_j(\nu)$ is also a periodic function of ν.

Eqs. (10.210) and (10.225) are the boundary conditions for the nonconformal multilayer film stack. For the conformal multilayer film stack, $\Delta' = 0$, and Eq. (10.225) reduces to

$$\hat{G}^{j+1} = \hat{G}^j \tag{10.226}$$

as expected.

The alert reader at this point may be uncomfortable with the manner in which we have matched fields at the interface between nonconformal grooves. We are essentially making a one-to-one matching of the Fourier components of the field amplitudes across the interface, albeit making sure that we are matching tangential components. This approach is known as the Rayleigh approximation. It has been shown that this approximation fails when the the groove depth becomes an appreciable fraction of a wavelength. The reason for this failure is that the fields in the region above the grating can be expanded in a Fourier series, but the fields within the grooves cannot, due to the evanescent components. Similarly, when the grooves are not conformal, the upper interface of layer j is a grating *within the transformed coordinate system of layer j*. Therefore, to properly handle the field within layer j at the upper interface, we should really transform each field component within layer j into the coordinate system of layer j+1 and then apply the matching boundary conditions. Essentially each diffracted component in the Fourier series expansion of the field within layer j must be expanded in another Fourier series at the upper interface of this layer to properly account for all the field amplitudes within the groove region at this interface. L. Li was the first to point out this issue. [37]

10.5.8 Transfer matrix for nonconformal thin films

Now that the boundary conditions have been obtained, we can apply them explicitly to the fields on both sides of each interface. We consider first the $\hat{F}$ field and then the $\hat{G}$ field. It is convenient to expand Eq. (10.104) as

$$\vec{\zeta}^{\,j}(u_j) = \begin{pmatrix} \vec{\hat{\boldsymbol{F}}}^{\,j} \\ \vec{\hat{\boldsymbol{G}}}^{\,j} \end{pmatrix} = \tilde{\mathrm{M}}^j\, \tilde{\boldsymbol{\Phi}}^j(u_j)\, \vec{\boldsymbol{b}}^{\,j} = \begin{pmatrix} \tilde{\mathrm{M}}^j(+) \\ \tilde{\mathrm{M}}^j(-) \end{pmatrix} \tilde{\boldsymbol{\Phi}}^j(u_j)\, \vec{\boldsymbol{b}}^{\,j} \tag{10.227}$$

where $\tilde{\mathrm{M}}^j(+)$ is the upper half of matrix $\tilde{\mathrm{M}}^j$, and $\tilde{\mathrm{M}}^j(-)$ is the lower half. Both are rectangular matrices of dimension 2N+1 rows by 4N+2 columns. So

$$\vec{\hat{\boldsymbol{F}}}^j\left(u_j\right) = \tilde{\mathrm{M}}^j(+)\,\tilde{\boldsymbol{\Phi}}^j\left(u_j\right)\vec{\boldsymbol{b}}^j \tag{10.228}$$

or from Eq. (10.109),

$$\hat{F}_p^j\left(u_j\right) = \sum_q M_{pq}^j(+)\exp\left(i\,r_q^j\,e_j\right)\exp\left(i\,r_q^j\,\Delta_j\right)b_q^j, \tag{10.229}$$

and

$$\vec{\hat{\boldsymbol{G}}}^j\left(u_j\right) = \tilde{\mathrm{M}}^j(-)\,\tilde{\boldsymbol{\Phi}}^j\left(u_j\right)\vec{\boldsymbol{b}}^j \tag{10.230}$$

or

$$\hat{G}_p^j\left(u_j\right) = \sum_q M_{pq}^j(-)\exp\left(i\,r_q^j\,e_j\right)\exp\left(i\,r_q^j\,\Delta_j\right)b_q^j. \tag{10.231}$$

Matching the $\hat{F}$ field at the interface using Eqs. (10.66) and (10.210),

$$\hat{F}^{j+1}\left(u_{j+1},\,v\right) =$$
$$\sum_m \hat{F}_m^{j+1}\left(u_{j+1}\right)\exp(i\,\alpha_m\,v) = \sum_m \hat{F}_m^j\left(u_j\right)\exp(i\,\alpha_m\,v) = \hat{F}^j\left(u_j,\,v\right). \tag{10.232}$$

where $u_{j+1} = d_{j+1}$ and $u_j = d_{j+1} + \Delta_j$ (and Δ_j is defined for each line segment of the groove profile in Eq. (10.6) and is zero if the films are conformal). Substituting Eq. (10.229) into this equation gives

$$\sum_{m,q} M_{mq}^{j+1}(+)\,\exp(i\,\alpha_m\,v)\,b_q^{j+1}$$
$$= \sum_{m,q} M_{mq}^{j}(+)\,\exp\left(i\,r_q^j\,e_j\right)\exp\left(i\,r_q^j\,\Delta_j\right)\exp(i\,\alpha_m\,v)\,b_q^j.$$

The factor $\exp\left(i\,r_q^j\,\Delta_j\right)$ on the right hand side of Eq. (10.233), not present with conformal films, is periodic with the grating and was previously expanded in a Fourier series in Eq. (10.9). Substituting this into Eq. (10.233) gives

$$\sum_{mq} M_{mq}^{j+1}(+)\,\exp(i\,\alpha_m\,v)\,b_q^{j+1}$$
$$= \sum_{m,q} M_{mq}^{j}(+)\sum_n L_n^j\left(r_q\right)\exp(i\,n\,K\,v)\,\exp\left(i\,r_q^j\,e_j\right)\exp(i\,\alpha_m\,v)\,b_q^j \tag{10.234}$$

$$= \sum_{mnq} M_{mq}^{j}(+)\,L_n^j\left(r_q\right)\exp\left(i\,r_q^j\,e_j\right)\exp(i\,\alpha_{m+n}\,v)\,b_q^j. \tag{10.235}$$

Replacing n with $n - m$,

$$= \sum_{mnq} M_{mq}^{j}(+)\,L_{n-m}^j\left(r_q\right)\exp\left(i\,r_q^j\,e_j\right)\exp(i\,\alpha_n\,v)\,b_q^j \tag{10.236}$$

and then swapping m and n,

$$= \sum_{mnq} M_{nq}^{j}(+)\,L_{m-n}^j\left(r_q\right)\exp\left(i\,r_q^j\,e_j\right)\exp(i\,\alpha_m\,v)\,b_q^j. \tag{10.237}$$

We can now equate term-by-term on both sides of the equality,

$$\sum_q M_{mq}^{j+1}(+)\,b_q^{j+1} = \sum_{nq} M_{nq}^{j}(+)\,L_{m-n}^j\left(r_q\right)\exp\left(i\,r_q^j\,e_j\right)b_q^j. \tag{10.238}$$

We can define the new rectangular matrix with 2N+1 rows and 4N+2 columns, $\tilde{\boldsymbol{X}}^{j}(+)$, where

$$X^{j}_{nq}(+) = \sum_{m} M^{j}_{mq}(+)\, L^{j}_{n-m}\left(r^{j}_{q}\right). \tag{10.239}$$

and the square diagonal phase matrix of rank 4N+2,

$$\Gamma^{j}_{mq} = \exp\left(i\, r^{j}_{q}\, e_{j}\right) \delta_{mq} \tag{10.240}$$

as defined in Eq. (10.106). Then Eq. (10.238) can be written

$$\tilde{\boldsymbol{M}}^{j+1}(+)\, \vec{\boldsymbol{b}}^{j+1} = \tilde{\boldsymbol{X}}^{j}(+)\, \tilde{\boldsymbol{\Gamma}}^{j}\, \vec{\boldsymbol{b}}^{j}. \tag{10.241}$$

This is the result for nonconformal films that corresponds to the top half of the matrix equation for conformal films, Eq. (10.193). We see that the top half of matrix $\tilde{\boldsymbol{M}}^{j}$ on the right hand side of Eq. (10.193) has been replaced by $\tilde{\boldsymbol{X}}^{j}(+)$ in Eq. (10.241). This makes sense since as seen in Eq. (10.21), the function L^{j}_{n-m} is zero when the films are conformal except for $n - m = 0$, when $L^{j}_{n-m} = 1$.

A similar relation must be obtained for the $\hat{G}$ field amplitudes. Substituting Eqs. (10.17), (10.18), (10.67), and (10.68) into the boundary condition Eq. (10.225),

$$\begin{aligned} &\sum_{m} \hat{G}^{j+1}_{m}(u) \exp(i\, \alpha_{m}\, v) \\ &= \left(\Delta'_{j} \sum_{p} d_{\mathrm{pj}} \exp(i\, p\, K\, x) + 1\right) \sum_{m} \hat{G}^{j}_{m}(u) \exp(i\, \alpha_{m}\, v) \\ &+ i\, \Delta'_{j}\, \eta_{j} \sum_{p} c_{pj} \exp(i\, p\, K\, x) \sum_{m} i\, \alpha_{m}\, F^{j}_{m}(u) \exp(i\, \alpha_{m}\, v). \end{aligned} \tag{10.242}$$

Substituting Eqs. (10.237) and (10.239) into (10.250) then gives

$$\sum_{mq} M_{mq}^{j+1}(-)\,\exp(i\,\alpha_m\,v)\,b_q^{j+1}$$

$$= \Delta_j' \sum_{mpq} d_{pj}\,\exp(i\,p\,K\,x)\,M_{mq}^{j}(-)\,\exp\left(i\,r_q^j\,e_j\right)\exp\left(i\,r_q^j\,\Delta_j\right)\exp(i\,\alpha_m\,v)\,b_q^j$$

$$+ \sum_{mq} M_{mq}^{j}(-)\,\exp\left(i\,r_q^j\,\Delta_j\right)\exp\left(i\,r_q^j\,e_j\right)\exp(i\,\alpha_m\,v)\,b_q^j - \Delta_j'\,\eta_j \sum_{mpq} \alpha_m\,c_{pj}$$

$$M_{mq}^{j}(+)\,\exp(i\,p\,K\,x)\,\exp\left(i\,r_q^j\,e_j\right)\exp\left(i\,r_q^j\,\Delta_j\right)\exp(i\,\alpha_m\,v)\,b_q^j.$$

Now, from Eq. (10.9),

$$\exp\left[i\,r_q^j\,\Delta_j(v)\right]\exp(i\,\alpha_m\,v) = \sum_s L_s^j\left(r_q\right)\exp(i\,\alpha_{m+s}\,v) \tag{10.244}$$

$$= \sum_s L_{s-m}^j\left(r_q\right)\exp(i\,\alpha_s\,v) \tag{10.245}$$

Differentiating both sides with respect to v, and substituting Eq. (10.245) back in for one term,

$$i\,r_q^j\,\Delta_j'\,\exp\left[i\,r_q^j\,\Delta_j(v)\right]\exp(i\,\alpha_m\,v) + i\,\alpha_m \sum_s L_{s-m}^j\left(r_q\right)\exp(i\,\alpha_s\,v) = \sum_s i\,\alpha_s\,L_{s-m}^j\left(r_q\right)\exp(i\,\alpha_s\,v) \tag{10.246}$$

or

$$\Delta_j'\,\exp\left[i\,r_q^j\,\Delta_j(v)\right]\exp(i\,\alpha_m\,v) = \frac{1}{r_q^j}\sum_s (\alpha_s - \alpha_m)\,L_{s-m}^j\left(r_q\right)\exp(i\,\alpha_s\,v) \tag{10.247}$$

$$= \frac{1}{r_q^j}\sum_s (s-m)\,K\,L_{s-m}^j\left(r_q\right)\exp(i\,\alpha_s\,v). \tag{10.248}$$

We can use Eq. (10.248) to eliminate Δ'_j in Eq. (10.243), and Eq. (10.9) to eliminate Δ_j,

$$\begin{aligned}
&\sum_{mq} M_{mq}^{j+1}(-)\exp(i\,\alpha_m\,v)\,b_q^{j+1} = \\
&\sum_p d_{pj}\exp(i\,p\,K\,v)\sum_{mqs}\frac{1}{r_q^j}\,M_{mq}^j(-)\,(s-m)\,K \\
&L_{s-m}^j(r_q)\exp\left(i\,r_q^j\,e_j\right)\exp(i\,\alpha_s\,v)\,b_q^j \\
&+\sum_{mq} M_{mq}^j(-)\exp\left(i\,r_q^j\,e_j\right)\sum_n L_n^j(r_q)\exp(i\,\alpha_{m+n}\,v)\,b_q^j - \eta_j \\
&\sum_p c_{pj}\exp(i\,p\,K\,v) \\
&\sum_{mqs}\frac{\alpha_m}{r_q^j}\,M_{mq}^j(+)\,(s-m)\,K\,L_{s-m}^j(r_q)\exp\left(i\,r_q^j\,e_j\right)\exp(i\,\alpha_s\,v)\,b_q^j.
\end{aligned} \tag{10.249}$$

In the first and third terms on the right hand side, let $s \to n - p$, and in the second term let $n \to n - m$,

$$\begin{aligned}
&= \sum_p d_{pj}\exp(i\,p\,K\,v)\sum_{mnq}\frac{1}{r_q^j}\,M_{mq}^j(-) \\
&(n-m-p)\,K\,L_{n-m-p}^j(r_q)\exp\left(i\,r_q^j\,e_j\right)\exp\left(i\,\alpha_{n-p}\,v\right)b_q^j \\
&+\sum_{mnq} M_{mq}^j(-)\,L_{n-m}^j(r_q)\exp\left(i\,r_q^j\,e_j\right)\exp(i\,\alpha_n\,v)\,b_q^j \\
&-\eta_j\sum_p c_{pj}\exp(i\,p\,K\,v)\sum_{mnq}\frac{\alpha_m}{r_q^j}\,M_{mq}^j(+)\,(n-m-p) \\
&K\,L_{n-m-p}^j(r_q)\exp\left(i\,r_q^j\,e_j\right)\exp\left(i\,\alpha_{n-p}\,v\right)b_q^j
\end{aligned} \tag{10.250}$$

and swap m and n in all the terms on the right hand side, and combine the exponential factors,

$$= \sum_p d_{pj}$$

$$\sum_{mnq} \frac{1}{r_q^j} M_{nq}^j(-)\,(m-n-p)\,K\,L_{m-n-p}^j\left(r_q\right)\exp\left(i\,r_q^j\,e_j\right)\exp(i\,\alpha_m\,v)\,b_q^j$$

$$+\sum_{mnq} M_{nq}^j(-)\,L_{m-n}^j\left(r_q\right)\exp\left(i\,r_q^j\,e_j\right)\exp(i\,\alpha_m\,v)\,b_q^j$$

$$-\eta_j\sum_p c_{pj}\sum_{mnq}\frac{\alpha_n}{r_q^j}\,M_{nq}^j(+)\,(m-n-p)$$

$$K\,L_{m-n-p}^j\left(r_q\right)\exp\left(i\,r_q^j\,e_j\right)\exp(i\,\alpha_m\,v)\,b_q^j.$$

We can now set the $\exp(i\,\alpha_m\,v)$ Fourier components equal to each other on right and left sides term-by-term, and we again swap m and n in the terms on the right hand side,

$$\sum_q M_{mq}^{j+1}(-)\,b_q^{j+1}$$

$$= K\sum_{pmq}\frac{d_{pj}}{r_q^j}\,M_{mq}^j(-)\,(n-m-p)\,L_{n-m-p}^j\left(r_q\right)\exp\left(i\,r_q^j\,e_j\right)b_q^j$$

$$+\sum_q M_{mq}^j(-)\,L_{n-m}^j\left(r_q\right)\exp\left(i\,r_q^j\,e_j\right)b_q^j$$

$$-K\,\eta_j\sum_{pmq} c_{pj}\,\frac{\alpha_m}{r_q^j}\,M_{mq}^j(+)\,(n-m-p)\,L_{n-m-p}^j\left(r_q\right)\exp\left(i\,r_q^j\,e_j\right)b_q^j. \qquad (10.252)$$

We now define the rectangular matrix $\tilde{\boldsymbol{X}}^j(-)$ with 2N+1 rows and 4N+2 columns,

$$X_{nq}^j(-) = \sum_m M_{mq}^j(-)\,L_{n-m}^j\left(r_q^j\right) +$$

$$\frac{K}{r_q^j}\sum_{mp}(n-m-p)\left(d_{pj}\,M_{mq}^j(-) - \eta_j\,\alpha_m\,c_{pj}\,M_{mq}^j(+)\right)L_{n-m-p}^j\left(r_q^j\right). \qquad (10.253)$$

Eq. (10.252) simplifies to

$$\tilde{\boldsymbol{M}}^{j+1}(-)\,\vec{\tilde{\boldsymbol{b}}}^{j+1} = \tilde{\boldsymbol{X}}^{j}(-)\,\tilde{\boldsymbol{\Gamma}}^{j}_{q}\left(\boldsymbol{e}_{j}\right)\vec{\tilde{\boldsymbol{b}}}^{j}. \tag{10.254}$$

This is the result for nonconformal films that corresponds to the bottom half of the matrix equation for conformal films, Eq. (10.253). The bottom half of matrix $\tilde{\boldsymbol{M}}^{j}$ on the right hand side of Eq. (10.253) has been replaced by $\tilde{\boldsymbol{X}}^{j}(-)$ in Eq. (10.254). Because the function L_n^j is zero when the films are conformal except for $n = 0$, when $L_n^j = 1$, Eq. (10.253) is quickly seen to reduce to the conformal case.

Eqs. (10.241) and (10.254) can be combined into a single equation,

$$\tilde{\boldsymbol{M}}^{j+1}\,\vec{\tilde{\boldsymbol{b}}}^{j+1} = \tilde{\boldsymbol{X}}^{j}\,\tilde{\boldsymbol{\Gamma}}^{j}\,\vec{\tilde{\boldsymbol{b}}}^{j} \tag{10.255}$$

where $\tilde{\boldsymbol{X}}$ is a square matrix of rank 4N+2,

$$\tilde{\boldsymbol{X}}^{j} = \begin{pmatrix} \tilde{\boldsymbol{X}}^{j}(+) \\ \tilde{\boldsymbol{X}}^{j}(-) \end{pmatrix} \tag{10.256}$$

and $0 \le j \le Q$. Eq. (10.255) for nonconformal films is the counterpart to Eq. (10.193) for conformal films.

We can use Eq. (10.255) to generate the transfer matrix.

$$\tilde{\boldsymbol{M}}^{Q+1}\,\vec{\tilde{\boldsymbol{b}}}^{Q+1} = \tilde{\boldsymbol{X}}^{Q}\,\tilde{\boldsymbol{\Gamma}}^{Q}\,\vec{\tilde{\boldsymbol{b}}}^{Q} = \tilde{\boldsymbol{X}}^{Q}\,\tilde{\boldsymbol{\Gamma}}^{Q}(\tilde{\boldsymbol{M}}^{Q})^{-1}\,\tilde{\boldsymbol{X}}^{Q-1}\,\tilde{\boldsymbol{\Gamma}}^{Q-1}\,\vec{\tilde{\boldsymbol{b}}}^{Q-1} \tag{10.257}$$

$$= \tilde{\boldsymbol{X}}^{Q}\,\tilde{\boldsymbol{\Gamma}}^{Q}(\tilde{\boldsymbol{M}}^{Q})^{-1}\,\tilde{\boldsymbol{X}}^{Q-1}\,\tilde{\boldsymbol{\Gamma}}^{Q-1}\cdots(\tilde{\boldsymbol{M}}^{2})^{-1}\,\tilde{\boldsymbol{X}}^{1}\,\tilde{\boldsymbol{\Gamma}}^{1}(\tilde{\boldsymbol{M}}^{1})^{-1}\,\tilde{\boldsymbol{X}}^{0}\,\tilde{\boldsymbol{\Gamma}}^{0}\,\vec{\tilde{\boldsymbol{b}}}^{0}. \tag{10.258}$$

We define the new matrices,

$$\tilde{\boldsymbol{H}}^{j} = \tilde{\boldsymbol{X}}^{j}\,\tilde{\boldsymbol{\Gamma}}^{j}\,(\tilde{\boldsymbol{M}}^{j})^{-1} \tag{10.259}$$

so Eq. (10.258) becomes

$$\tilde{\boldsymbol{H}}\left(\tilde{\boldsymbol{X}}^{0}\,\vec{\tilde{\boldsymbol{b}}}^{0}\right) = \tilde{\boldsymbol{H}}^{Q}\,\tilde{\boldsymbol{H}}^{Q-1}\cdots\tilde{\boldsymbol{H}}^{1}\,\tilde{\boldsymbol{X}}^{0}\,\vec{\tilde{\boldsymbol{b}}}^{0} = \tilde{\boldsymbol{M}}^{Q+1}\,\vec{\tilde{\boldsymbol{b}}}^{Q+1} \tag{10.260}$$

where

$$\tilde{\boldsymbol{H}} \equiv \tilde{\boldsymbol{H}}^{Q}\,\tilde{\boldsymbol{H}}^{Q-1}\cdots\tilde{\boldsymbol{H}}^{2}\,\boldsymbol{H}^{1}. \tag{10.261}$$

Eq. (10.260) is the transfer matrix equation that expresses the field amplitudes inside the substrate, $\vec{\boldsymbol{b}}^0$, in terms of the field amplitudes in the incident medium, $\vec{\boldsymbol{b}}^{Q+1}$. At the bottom interface, $\Delta_0 = 0$, and

$$L^0_{m-n}(r_q) = \begin{cases} 1 & \text{for } m = n \\ 0 & \text{for } m \neq n \end{cases}. \tag{10.262}$$

Then

$$X^0_{nq}(+) = \sum_m M^0_{mq}(+)\, L^0_{m-n}(r_q) = M^0_{nq}(+) \tag{10.263}$$

and

$$X^0_{nq}(-) = \sum_m M^0_{mq}(-)\, L^0_{m-n}(r_q) + \frac{K}{r_q^j} \sum_{mp} (n-m-p) \left(d_{pj}\, M^0_{mq}(-) - \eta_j\, \alpha_m\, c_{pj}\, M^0_{mq}(+)\right) L^0_{n-m-p}(r_q) \tag{10.264}$$

$$= M^0_{nq}(-). \tag{10.265}$$

Therefore, within the substrate,

$$\tilde{\boldsymbol{X}}^0\, \vec{\boldsymbol{b}}^0 = \tilde{\boldsymbol{M}}^0\, \vec{\boldsymbol{b}}^0, \tag{10.266}$$

which is the total field in the substrate. The transfer matrix Eq. (10.260) is solved in exactly the same manner as was discussed for conformal thin films with the matrix definition in Eq. (10.259) rather than Eq. (10.197).

A simpler expression for Eq. (10.253) has been given by Li. [37]

10.5.9 Scattering matrix

Although we have now derived the complete technique for solving the vector diffraction problem of a multilayer thin film stack with nonformal gratings at each layer, one finds that these equations exhibit numerical instability when the films become too thick or the grooves too deep due to the exponential dependence of the evanescent field amplitudes and the finite precision of the machine computation. It is relatively straightforward to convert the transfer matrix formalism, in which the fields on one side of an interface are related to the fields on the other side of the interface, into a scattering matrix formalism in which the fields incident upon the interface from above and below are related to the fields reflected from the interface into the upper and lower media. It turns out that this approach eliminates the problems in loss of precision caused by the exponentials in the calculation. We follow the procedure described by Cotter *et al.* [38]

With reference to Fig. 10.33 we can denote the 2N+1 field amplitudes for which $\mathrm{Re}(r_q) > 0$, corresponding to the "upward" propagating and evanescent fields, with a "+" subscript. Likewise, the 2N+1 field amplitudes for which $\mathrm{Re}(r_q) < 0$, corresponding to the "downward" propagating and evanscent fields, are denoted with a "-" subscript.

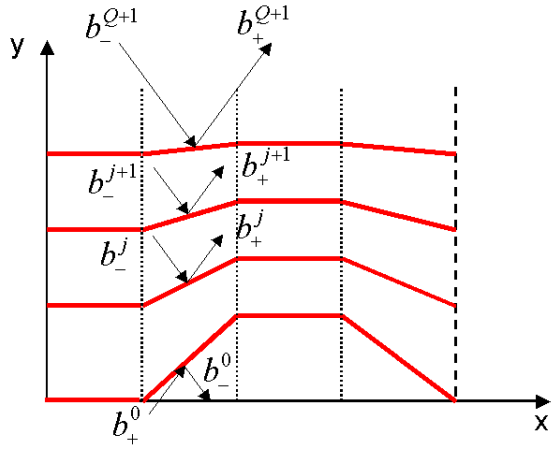

Fig. 10.33. Diagram showing upward (+) and downward (-) propagating modes at each interface.

Let us now define a scattering matrix $\tilde{\boldsymbol{S}}^j$ which connects the 2N+1 field amplitudes which are incident upon the bottom interface, $\vec{\boldsymbol{b}}_+^0$, and the 2N+1 field amplitudes which are incident upon *j*'th interface, $\vec{\boldsymbol{b}}_-^j$, to the 2N+1 field amplitudes which are reflected from the bottom interface, $\vec{\boldsymbol{b}}_-^0$, and the 2N+1 field amplitudes which are reflected from the *j*'th interface, $\vec{\boldsymbol{b}}_+^j$,

$$\begin{pmatrix} \vec{b}_+^{\,j} \\ \vec{b}_-^{\,0} \end{pmatrix} = \begin{pmatrix} \tilde{S}_{11}^{j} & \tilde{S}_{12}^{j} \\ \tilde{S}_{21}^{j} & \tilde{S}_{22}^{j} \end{pmatrix} \begin{pmatrix} \vec{b}_+^{\,0} \\ \vec{b}_-^{\,j} \end{pmatrix}. \tag{10.267}$$

The eigenvalues r_q associated with each column in the transfer matrix, Eq. (10.263), for the 2N+1 "upward" modes satisfy either

$$\mathrm{Im}\left(r_q^j\right) = 0 \qquad \text{and} \qquad \mathrm{Re}\left(r_q^j\right) > 0 \tag{10.268}$$

for the propagating modes, or

$$\mathrm{Im}\left(r_q^{Q+1}\right) > 0 \tag{10.269}$$

for the evanescent modes. We rearrange columns in $\tilde{\boldsymbol{X}}^{\,j}$ so that the upward propagating modes are the left-most columns of the matrix. The remaining columns in the left half of the transfer matrix are associated with the evanescent modes. Similarly, there are 2N+1 "downward" modes. The eigenvalues associated with the column vectors in the transfer matrix for the downward modes satisfy

$$\mathrm{Im}\left(r_q^j\right) = 0 \qquad \text{and} \qquad \mathrm{Re}\left(r_q^j\right) < 0 \tag{10.270}$$

for the propagating modes, or

$$\mathrm{Im}\left(r_q^{Q+1}\right) < 0 \tag{10.271}$$

for the evanescent modes. The column vectors associated with the downward propagating modes are placed on the left side of the right half of the transfer matrix. Finally, the remaining column vectors in the right side of the transfer matrix are associated with the downward evanescent modes. We can then write Eq. (10.263) as

$$\tilde{\boldsymbol{M}}^{\,j+1} \begin{pmatrix} \vec{b}_+^{\,j+1} \\ \vec{b}_-^{\,j+1} \end{pmatrix} = \tilde{\boldsymbol{X}}^{\,j}\, \tilde{\boldsymbol{\Gamma}}^{j} \begin{pmatrix} \vec{b}_+^{\,j} \\ \vec{b}_-^{\,j} \end{pmatrix} \tag{10.272}$$

where the matrix $\tilde{\Phi}^{j}$ has also been appropriately computed according to Eq. (10.248). Solving for the amplitude vector on the right hand side of this equation,

$$\begin{pmatrix} \vec{b}_+^{\,j} \\ \vec{b}_-^{\,j} \end{pmatrix} = \begin{pmatrix} \tilde{W}_{11}^{j} & \tilde{W}_{12}^{j} \\ \tilde{W}_{21}^{j} & \tilde{W}_{22}^{j} \end{pmatrix} \begin{pmatrix} \vec{b}_+^{\,j+1} \\ \vec{b}_-^{\,j+1} \end{pmatrix} \tag{10.273}$$

where we have defined the new transfer matrix,

$$\tilde{\boldsymbol{W}}^{j} \equiv \left(\tilde{\boldsymbol{X}}^{j}\,\tilde{\boldsymbol{\Gamma}}^{j}\right)^{-1}\tilde{\boldsymbol{M}}^{j+1} = \left(\tilde{\boldsymbol{\Gamma}}^{j}\right)^{-1}\left(\tilde{\boldsymbol{X}}^{j}\right)^{-1}\tilde{\boldsymbol{M}}^{j+1}. \tag{10.274}$$

We also note that at the bottom interface with the substrate, by virtue of Eqs. (10.186) and (10.266), we can reduce Eq. (10.272) to

$$\tilde{\boldsymbol{M}}^{1}\begin{pmatrix}\vec{\boldsymbol{b}}_{+}^{1}\\ \vec{\boldsymbol{b}}_{-}^{1}\end{pmatrix} = \tilde{\boldsymbol{M}}^{0}\begin{pmatrix}\vec{\boldsymbol{b}}_{+}^{0}\\ \vec{\boldsymbol{b}}_{-}^{0}\end{pmatrix} = \tilde{\boldsymbol{M}}_{s}\begin{pmatrix}\vec{\boldsymbol{b}}_{+}^{0}\\ \vec{\boldsymbol{b}}_{-}^{0}\end{pmatrix} \tag{10.275}$$

so

$$\begin{pmatrix}\vec{\boldsymbol{b}}_{+}^{0}\\ \vec{\boldsymbol{b}}_{-}^{0}\end{pmatrix} = \begin{pmatrix}\tilde{\boldsymbol{W}}_{11}^{0} & \tilde{\boldsymbol{W}}_{12}^{0}\\ \tilde{\boldsymbol{W}}_{21}^{0} & \tilde{\boldsymbol{W}}_{22}^{0}\end{pmatrix}\begin{pmatrix}\vec{\boldsymbol{b}}_{+}^{1}\\ \vec{\boldsymbol{b}}_{-}^{1}\end{pmatrix} \tag{10.276}$$

where

$$\tilde{\boldsymbol{W}}^{0} \equiv \left(\tilde{\boldsymbol{M}}_{s}\right)^{-1}\tilde{\boldsymbol{M}}^{1}. \tag{10.277}$$

We now want to find the components of the scattering matrix for the $(j+1)^{\text{st}}$ interface, $\tilde{\boldsymbol{S}}^{j+1}$, in terms of $\tilde{\boldsymbol{S}}^{j}$ and $\tilde{\boldsymbol{W}}^{j}$. Eqs. (10.275) and (10.276) can be expanded into the four equations

$$\vec{\boldsymbol{b}}_{+}^{j} = \tilde{\boldsymbol{S}}_{11}^{j}\,\vec{\boldsymbol{b}}_{+}^{0} + \tilde{\boldsymbol{S}}_{12}^{j}\,\vec{\boldsymbol{b}}_{-}^{j} \tag{10.278}$$

$$\vec{\boldsymbol{b}}_{-}^{0} = \tilde{\boldsymbol{S}}_{21}^{j}\,\vec{\boldsymbol{b}}_{+}^{0} + \tilde{\boldsymbol{S}}_{22}^{j}\,\vec{\boldsymbol{b}}_{-}^{j} \tag{10.279}$$

$$\vec{\boldsymbol{b}}_{+}^{j} = \tilde{\boldsymbol{W}}_{11}^{j}\,\vec{\boldsymbol{b}}_{+}^{j+1} + \tilde{\boldsymbol{W}}_{12}^{j}\,\vec{\boldsymbol{b}}_{-}^{j+1} \tag{10.280}$$

$$\vec{\boldsymbol{b}}_{-}^{j} = \tilde{\boldsymbol{W}}_{21}^{j}\,\vec{\boldsymbol{b}}_{+}^{j+1} + \tilde{\boldsymbol{W}}_{22}^{j}\,\vec{\boldsymbol{b}}_{-}^{j+1} \tag{10.281}$$

We eliminate the field amplitudes with the superscript j from these equations by equating Eqs. (10.278) and (10.280),

$$\tilde{S}_{11}^{j}\,\vec{b}_{+}^{0} + \tilde{S}_{12}^{j}\,\vec{b}_{-}^{j} = \tilde{W}_{11}^{j}\,\vec{b}_{+}^{j+1} + \tilde{W}_{12}^{j}\,\vec{b}_{-}^{j+1} \tag{10.282}$$

and by substituting $\vec{b}_{-}^{j}$ from Eq. (10.281) into Eqs. (10.279) and (10.282),

$$\vec{b}_{-}^{0} = \tilde{S}_{21}^{j}\,\vec{b}_{+}^{0} + \tilde{S}_{22}^{j}\left(\tilde{W}_{21}^{j}\,\vec{b}_{+}^{j+1} + \tilde{W}_{22}^{j}\,\vec{b}_{-}^{j+1}\right) \tag{10.283}$$

$$\tilde{S}_{11}^{j}\,\vec{b}_{+}^{0} + \tilde{S}_{12}^{j}\left(\tilde{W}_{21}^{j}\,\vec{b}_{+}^{j+1} + \tilde{W}_{22}^{j}\,\vec{b}_{-}^{j+1}\right) = \tilde{W}_{11}^{j}\,\vec{b}_{+}^{j+1} + \tilde{W}_{12}^{j}\,\vec{b}_{-}^{j+1}. \tag{10.284}$$

Rearranging terms gives

$$\vec{b}_{-}^{0} = \tilde{S}_{21}^{j}\,\vec{b}_{+}^{0} + \left(\tilde{S}_{22}^{j}\,\tilde{W}_{21}^{j}\right)\vec{b}_{+}^{j+1} + \left(\tilde{S}_{22}^{j}\,\tilde{W}_{22}^{j}\right)\vec{b}_{-}^{j+1} \tag{10.285}$$

and

$$\left(\tilde{S}_{12}^{j}\,\tilde{W}_{21}^{j} - \tilde{W}_{11}^{j}\right)\vec{b}_{+}^{j+1} = \left(\tilde{W}_{12}^{j} - \tilde{S}_{12}^{j}\,\tilde{W}_{22}^{j}\right)\vec{b}_{-}^{j+1} - \tilde{S}_{11}^{j}\,\vec{b}_{+}^{0}. \tag{10.286}$$

This last equation is rewritten

$$\begin{aligned}\vec{b}_{+}^{j+1} = {} & \left[\left(\tilde{S}_{12}^{j}\,\tilde{W}_{21}^{j} - \tilde{W}_{11}^{j}\right)^{-1}\left(\tilde{W}_{12}^{j} - \tilde{S}_{12}^{j}\,\tilde{W}_{22}^{j}\right)\right] \\ & \vec{b}_{-}^{j+1} - \left[\left(\tilde{S}_{12}^{j}\,\tilde{W}_{21}^{j} - \tilde{W}_{11}^{j}\right)^{-1}\tilde{S}_{11}^{j}\right]\vec{b}_{+}^{0}.\end{aligned} \tag{10.287}$$

Now we can eliminate the $\vec{b}_{+}^{j+1}$ term in Eq. (10.285) using Eq. (10.287),

$$\vec{b}_-^{\,0} = \left[\tilde{S}_{21}^{j} - \left(\tilde{S}_{22}^{j}\,\tilde{W}_{21}^{j}\right)\left(\tilde{S}_{12}^{j}\,\tilde{W}_{21}^{j} - \tilde{W}_{11}^{j}\right)^{-1}\tilde{S}_{11}^{j}\right]\vec{b}_+^{\,0} + \left[\left(\tilde{S}_{22}^{j}\,\tilde{W}_{21}^{j}\right)\left(\tilde{S}_{12}^{j}\,\tilde{W}_{21}^{j} - \tilde{W}_{11}^{j}\right)^{-1}\left(\tilde{W}_{12}^{j} - \tilde{S}_{12}^{j}\,\tilde{W}_{22}^{j}\right) + \left(\tilde{S}_{22}^{j}\,\tilde{W}_{22}^{j}\right)\right]\vec{b}_-^{\,j+1}$$

Now, the scattering matrix for layer j+1 provides two additional matrix equations,

$$\vec{b}_+^{\,j+1} = \tilde{S}_{11}^{j+1}\,\vec{b}_+^{\,0} + \tilde{S}_{12}^{j+1}\,\vec{b}_-^{\,j+1} \tag{10.289}$$

and

$$\vec{b}_-^{\,0} = \tilde{S}_{21}^{j+1}\,\vec{b}_+^{\,0} + \tilde{S}_{22}^{j+1}\,\vec{b}_-^{\,j+1}\,. \tag{10.290}$$

Comparison of Eq. (10.287) with Eq. (10.289) immediately gives

$$\tilde{S}_{11}^{j+1} = \left(\tilde{W}_{11}^{j} - \tilde{S}_{12}^{j}\,\tilde{W}_{21}^{j}\right)^{-1}\tilde{S}_{11}^{j} \tag{10.291}$$

and

$$\tilde{S}_{12}^{j+1} = \left(\tilde{W}_{11}^{j} - \tilde{S}_{12}^{j}\,\tilde{W}_{21}^{j}\right)^{-1}\left(\tilde{S}_{12}^{j}\,\tilde{W}_{22}^{j} - \tilde{W}_{12}^{j}\right). \tag{10.292}$$

Comparison of Eq. (10.290) with Eq. (10.288), and making use of Eqs. (10.291) and (10.292) to simplify the notation, we find

$$\tilde{S}_{21}^{j+1} = \tilde{S}_{21}^{j} - \left(\tilde{S}_{22}^{j}\,\tilde{W}_{21}^{j}\right)\left(\tilde{S}_{12}^{j}\,\tilde{W}_{21}^{j} - \tilde{W}_{11}^{j}\right)^{-1}\tilde{S}_{11}^{j} = \tilde{S}_{21}^{j} + \tilde{S}_{22}^{j}\,\tilde{W}_{21}^{j}\,\tilde{S}_{11}^{j+1} \tag{10.293}$$

and

$$\tilde{S}_{22}^{j+1} = \left(\tilde{S}_{22}^{j}\,\tilde{W}_{21}^{j}\right)\left(\tilde{S}_{12}^{j}\,\tilde{W}_{21}^{j} - \tilde{W}_{11}^{j}\right)^{-1}\left(\tilde{W}_{12}^{j} - \tilde{S}_{12}^{j}\,\tilde{W}_{22}^{j}\right) + \left(\tilde{S}_{22}^{j}\,\tilde{W}_{22}^{j}\right) = \tilde{S}_{22}^{j}\,\tilde{W}_{22}^{j} + \tilde{S}_{22}^{j}\,\tilde{W}_{21}^{j}\,\tilde{S}_{12}^{j+1}\,. \tag{10.294}$$

Eqs. (10.291) - (10.294) determine the $(j+1)^{st}$ scattering matrix in terms of the j^{th} scattering and transfer matrices. Starting with $\tilde{\boldsymbol{S}}^0$, the identity matrix, once the transfer matrices have been determined for each layer, we can successively determine the scattering matrix for each layer until we reach $j = Q+1$, the upper dielectric medium. This final matrix connects the incident field amplitude $\vec{\boldsymbol{b}}_-^{Q+1}$ to the reflected field amplitudes, $\vec{\boldsymbol{b}}_+^{Q+1}$, and transmitted field amplitudes, $\vec{\boldsymbol{b}}_-^{0}$.

$$\begin{pmatrix} \vec{\boldsymbol{b}}_+^{Q+1} \\ \vec{\boldsymbol{b}}_-^{0} \end{pmatrix} = \begin{pmatrix} \tilde{\boldsymbol{S}}_{11}^{Q+1} & \tilde{\boldsymbol{S}}_{12}^{Q+1} \\ \tilde{\boldsymbol{S}}_{21}^{Q+1} & \tilde{\boldsymbol{S}}_{22}^{Q+1} \end{pmatrix} \begin{pmatrix} \vec{\boldsymbol{b}}_+^{0} \\ \vec{\boldsymbol{b}}_-^{Q+1} \end{pmatrix}. \tag{10.295}$$

We note that the amplitudes denoted by the vector $\vec{\boldsymbol{b}}_+^{0}$ are all identically zero - there are no incident fields from below the substrate onto the thin film stack. Therefore, the reflected field amplitudes are

$$\vec{\boldsymbol{b}}_+^{Q+1} = \tilde{\boldsymbol{S}}_{12}^{Q+1} \vec{\boldsymbol{b}}_-^{Q+1} \tag{10.296}$$

and the transmitted field amplitudes are

$$\vec{\boldsymbol{b}}_-^{0} = \tilde{\boldsymbol{S}}_{22}^{Q+1} \vec{\boldsymbol{b}}_-^{Q+1} . \tag{10.297}$$

In the paper by Priest *et al.*, [32] there is an additional somewhat complex procedure described for converting these results into reflectivity and transmissivity amplitudes. However, because we have already employed the procedure of Chandezon to rewrite the reflected and transmitted field amplitudes as sums of propagating plane waves and evanescent modes, Eqs. (10.296) and (10.297) are in fact the final result. In particular, the first component of $\vec{\boldsymbol{b}}_-^{Q+1}$ is unity for the amplitude of the incident plane wave, and all other components are zero. Therefore, the first column of $\tilde{\boldsymbol{S}}_{12}^{Q+1}$ is composed of the amplitude components for all the reflected orders, and the first column of $\tilde{\boldsymbol{S}}_{22}^{Q+1}$ is composed of the amplitude components for all the transmitted orders.

When computing reflected and transmitted *intensities* for each diffracted order, it is

useful to consider the component of the Poynting vector along the *y*-direction. This component will be proportional to $n \cdot |E|^2 \cos(\theta_m)$ or $|H|^2 \cos(\theta_m)/n$ where θ_m is the polar angle of the diffracted order and n is the refractive index of the medium. For TE mode we are solving for the electric field amplitude, so we use the first of these functions to obtain the field intensity for both the diffracted order and the incident plane wave, while for TM mode we are solving for the magnetic field amplitude so we use the second of these functions to do the same thing. We then normalize the diffracted intensity by the incident intensity to obtain the reflectivity and/or transmissivity of the grating film stack for each order.

The scattering matrices can also be used to find the field amplitudes within each layer. Eqs. (10.289) and (10.290) with $\vec{b}_+^0 = 0$ become

$$\vec{\boldsymbol{b}}_+^j = \tilde{\boldsymbol{S}}_{12}^j \vec{\boldsymbol{b}}_-^j \tag{10.298}$$

and

$$\vec{\boldsymbol{b}}_-^0 = \tilde{\boldsymbol{S}}_{22}^j \vec{\boldsymbol{b}}_-^j \qquad \text{or} \qquad \vec{\boldsymbol{b}}_-^j = (\tilde{\boldsymbol{S}}_{22}^j)^{-1} \vec{\boldsymbol{b}}_-^0 . \tag{10.299}$$

Therefore, the total amplitude vector for layer *j* is a function of the scattering matrix for that layer and the transmitted amplitude vector,

$$\vec{\boldsymbol{b}}^j = \begin{pmatrix} \tilde{\boldsymbol{S}}_{12}^j (\tilde{\boldsymbol{S}}_{22}^j)^{-1} \\ \\ (\tilde{\boldsymbol{S}}_{22}^j)^{-1} \end{pmatrix} \cdot \begin{pmatrix} \vec{\boldsymbol{b}}_-^0 \\ \vec{\boldsymbol{b}}_-^0 \end{pmatrix}. \tag{10.300}$$

10.5.10 Field profile

Once the components of the $\vec{\boldsymbol{b}}$ scattering amplitude vector have been computed for each layer, the field amplitude can be computed through the thickness of the film stack. We consider the F component of the vector $\vec{\zeta}$, which corresponds to the $\vec{\boldsymbol{E}}$ field for TE polarization and to $\gamma_1 \vec{\boldsymbol{H}}$ for TM polarization. For some arbitrary position on the *x* axis we can make use of the expansion in Eq. (10.66) to determine the field profile along the *y*-direction. However, for simplicity we will consider the field profile at $x = 0$. In that case,

$$F^j(u) = \sum_m F_m^j(u) \tag{10.301}$$

where the different components F_m are given by the top half of the $\vec{\zeta}$ vector. The $\vec{\zeta}$ vector is itself a summation of eigenvectors according to Eq. (10.101),

$$\vec{\zeta}^j = \sum_q b_q^j \, \hat{\boldsymbol{V}}_q^j \, e^{i \, r_q^j (u - d_j)} \tag{10.302}$$

so, in a given layer,

$$\begin{pmatrix} F_{-m} \\ F_{-m+1} \\ \vdots \\ F_{m-1} \\ F_m \end{pmatrix} = \tag{10.303}$$

$$\begin{pmatrix} b_1 M_{11} e^{i r_1 u} + b_2 M_{12} e^{i r_2 u} + ... + b_{4N+2} M_{1,4N+2} e^{i r_{4N+2} u} \\ b_1 M_{21} e^{i r_1 u} + b_2 M_{22} e^{i r_2 u} + ... + b_{4N+2} M_{2,4N+2} e^{i r_{4N+2} u} \\ \vdots \\ b_1 M_{2N,1} e^{i r_1 u} + b_2 M_{2N,2} e^{i r_2 u} + ... + b_{4N+2} M_{2N,4N+2} e^{i r_{4N+2} u} \\ b_1 M_{2N+1,1} e^{i r_1 u} + b_{2N+1,} M_{12} e^{i r_2 u} + ... + b_{4N+2} M_{2N+1,4N+2} e^{i r_{4N+2} u} \end{pmatrix}.$$

Combining Eq. (10.301) with Eq. (10.303) gives the total field in layer j at $x = 0$,

$$F^j = \sum_{n=1}^{4N+2} b_n^j \, e^{i \, r_n^j (u - d_j)} \sum_{m=1}^{2N+1} M_{mn}^j. \tag{10.304}$$

Exercises

1. Recognizing that ϵ'_m generally becomes more negative as the wavelength increases, what do you expect to happen to the SP wavevector with increasing wavelength? (see Eq. 10.2) What is the limiting value of k_{sp} as $\epsilon'_m \to -\infty$?

2. For what thickness of aluminum film is the Kretschmann configuration optimized at a incident wavelength of 900 nm?

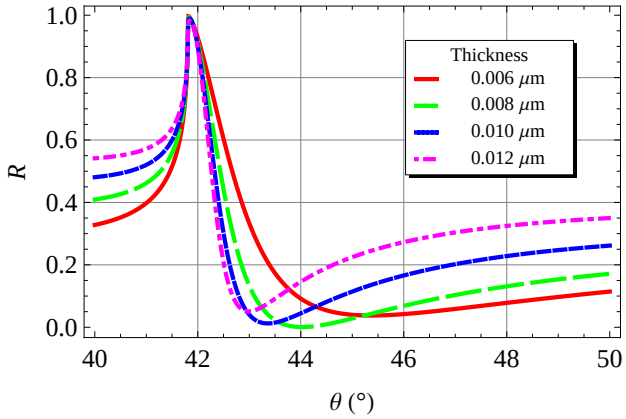

3. At a wavelength of 320 nm, the refractive index for silver is 0.765 + *i* 0.611. Is the reflectivity dip at this wavelength in Fig. 10.8 due to a SP resonance? At what silver thickness is this dip minimized?

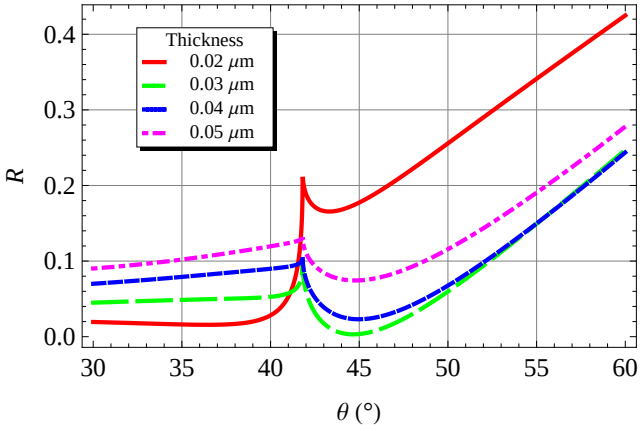

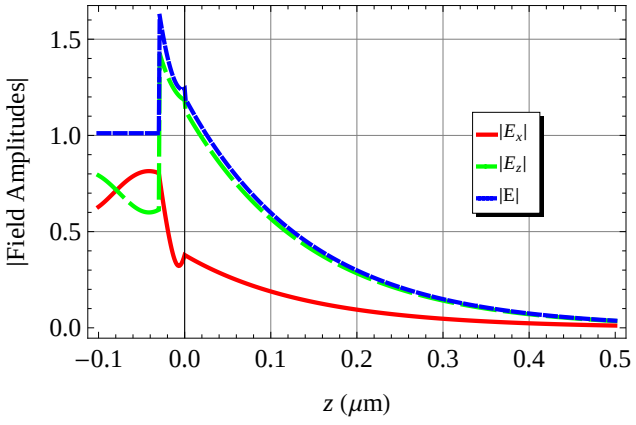

4. Is the component of the wavevector of an incident plane wave which lies in the plane of the surface larger or smaller for a larger angle of incidence? In light of the answer to question 1, if the angle of incidence is changed from 43° to 45° what should happen to the SP resonance wavelength in the Kretschmann configuration? Replot Fig. 10.8 for this new angle of incidence to verify your answer.

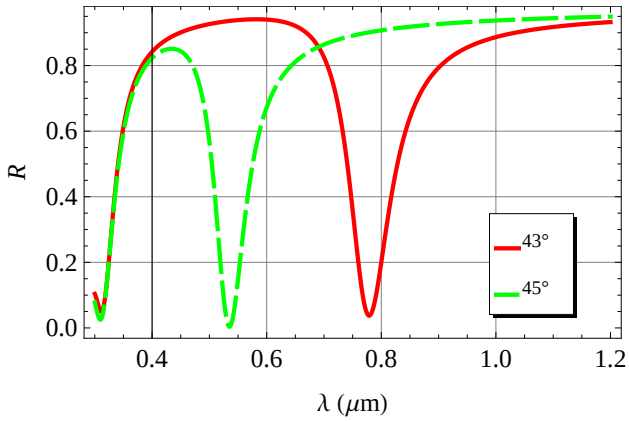

5. It was stated in the text that a low index dielectric like MgF_2 can be used in place of the air spacer in the Otto configuration. For MgF_2 with a refractive index of 1.38, what thickness of the dielectric film would give the largest dip in reflectivity for gold and at what angle of incidence is the SP excited?

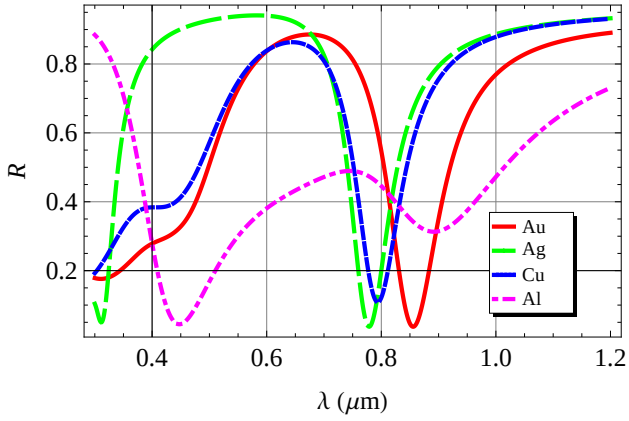

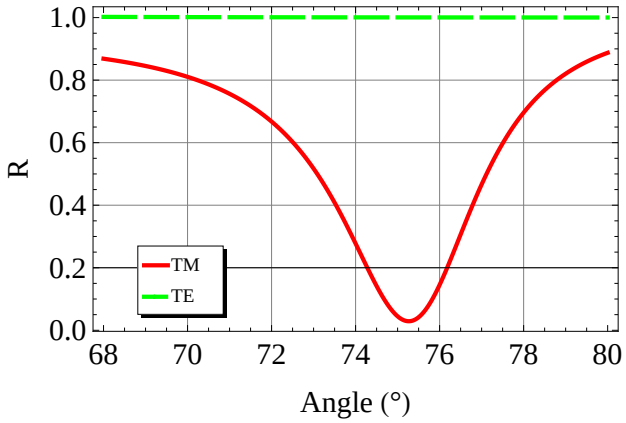

Fig. 10.4: Reflectivity of TE and TM polarization vs. angle of incidence for a 0.55 μm MgF_2 spacer in the Otto configuration. (*Mathematica* simulation.)

6. Explore the wavelength dependence of the coupling efficiency for gold, silver, aluminum and copper over the wavelength range of 300 nm to 1200 nm. What thickness of aluminum film gives optimal coupling?

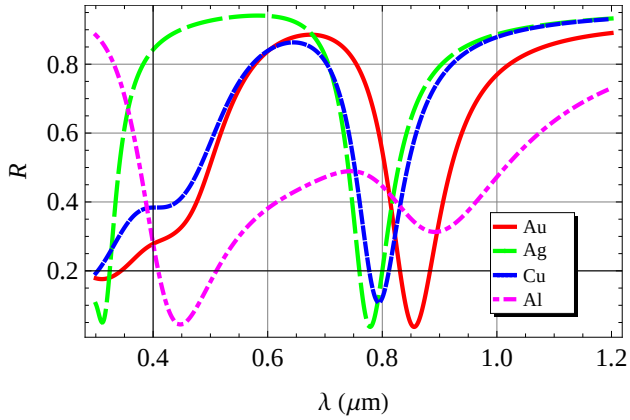

Exercise 6: Reflectivity of TM polarization vs. wavelength for various metal films in the Kretschmann configuration. The Ag, Au, and Cu films are 50 nm thick. The Al film is 18 nm thick. The dielectric below the metal film is air.

References

[1] A. Otto. Excitation of nonradiative surface plasma waves in silver by the method of frustrated total reflection. *Z. Phys.* **216** (1968) 398.

[2] E. Kretschmann and H. Raether. Radiative decay of nonradiative surface plasmons excited by light. *Z. Naturforsch.* **23a** (1968) 2135.

[3] H. Kano. Excitation of surface plasmon polaritons by a focused laser beam. In *Near-Field Optics and Surface Plasmon Polaritons,* ed. S. Kawata (New York: Springer, 2001) 189.

[4] R. W. Wood. On the remarkable case of uneven distribution of light in a diffraction grating spectrum. *Philos. Mag.* **4** (1902) 396.

[5] R. W. Wood. Anomalous diffraction gratings. *Phys. Rev.* **48** (1935) 928.

[6] Lord Rayleigh. Note on the remarkable case of diffraction spectra described by Prof. Wood. *Philos. Mag.* **14** (1907) 60.

[7] U. Fano. The theory of anomalous diffraction gratings and of quasi-stationary waves on metallic surfaces (Sommerfeld's waves). *J. Opt. Soc. Am.* **31** (1941) 213.

[8] A. D. Rakic, A. B. Djurišic, J. M. Elazar and M. L. Majewski. Optical properties of metallic films for vertical-cavity optoelectronic devices. *Appl. Opt.* **37** (1998) 5271.

[9] S. J. Elston, G. P. Bryan-Brown, T. W. Priest and J. R. Sambles. Surface-resonance polarization conversion mediated by broken surface symmetry. *Phys. Rev. B* **44** (1991) 3483.

[10] S. J. Elston, G. P. Bryan-Brown and J. R. Sambles. Polarization conversion from diffraction gratings. *Phys. Rev. B* **44** (1991) 6393.

[11] E. A. Stern. Plasma radiation by rough surfaces. *Phys. Rev. Lett.* **19** (1967) 1321.

[12] E. Kretschmann. The angular dependence and the polarisation of light emitted by surface plasmons on metals due to roughness. *Opt. Commun.* **5** (1972) 331

[13] E. Kretschmann. Die bestimmung der oberflächenrauhigkeit dünner schichten durch messung der winkelabhängigkeit der streustrahlung von oberflächenplasmaschwingungen. *Opt. Commun.* **10** (1974) 353.

[14] H. Raether, *Surface Plasmons on Smooth and Rough Surfaces and on Gratings* (Berlin: Springer, Berlin, 1988).

[15] K. Arya, Z. B. Su and J. L. Birman. Localization of the surface plasmon polariton caused by random roughness and its role in surface-enhanced optical phenomena. *Phys. Rev. Lett.* **54** (1985) 1559

[16] S. I. Bozhevolnyi, B. Vohnsen, I. I. Smolyaninov and A. V. Zayats. Direct observation of surface polariton localizaton caused by surface roughness. *Opt. Commun.* **117** (1995) 417.

[17] S. I. Bozhevolnyi. Localization phenomena in elastic surface-polariton scattering caused by surface roughness. *Phys. Rev. B* **54** (1996) 8177

[18] S. I. Bozhelvolnyi, I. I. Smolyaninov and A. V. Zayats. Near-field microscopy of surface-plasmon polaritons: Localization and internal interface imaging. *Phys. Rev. B* **51** (1995) 17916.

[19] G. I. Stegeman, R. F. Wallis and A. A. Maradudin. Excitation of surface polaritons by end-fire coupling. *Opt. Lett.* **8** (1983) 386.

[20] J. J. Burke, G. I. Stegeman and T. Tamir. Surface-polariton-like waves guided by thin, lossy metal films. *Phys. Rev. B* **33** (1986) 5186.

[21] R. Charbonneau, N. Lahoud and P. Berini. Demonstration of integrated optics elements based on long-range surface plasmon polaritons. *Opt. Exp.* **13** (2005) 977.

[22] Z. Sun and D. Zeng. Coupling of surface plasmon waves in metal/dielectric gap waveguides and single interface waveguides. *J. Opt. Soc. Am. B* **24** (2007) 2883.

[23] A. Degiron, S-Y. Cho, C. Harrison, N. M. Jokerst, C. Dellagiacoma, O. J. F. Martin and D. R. Smith. Experimental comparison between conventional and hybrid long-range surface plasmon waveguide bends. *Phys. Rev. A* **77** (2008) 021804.

[24] B. Hecht, H. Bielefeldt, L. Novotny, Y. Inouye, and D. W. Pohl. Local excitation,

scattering, and interference of surface plasmons. *Phys. Rev. Lett.* **77** (1996) 1889.

[25] H. Ditlbacher, J. R. Krenn, G. Schider, A. Leitner and F. R. Aussenegg. Two-dimensional optics with surface plasmon polaritons. *Appl. Phys. Lett.* **81** (2002) 1762.

[26] S. Kim, Y. Lim, H. Kim, J. Park, and B. Lee. Optical beam focusing by a single subwavelength metal slit surrounded by chirped dielectric surface gratings. *Appl. Phys. Lett.* **92** (2008) 013103.

[27] Y. S. Jung, J. Wuenschell, T. Schmidt, and H. K. Kim. Near- to far-field imaging of free-space and surface-bound waves emanating from a metal nanoslit. *Appl. Phys. Lett.* **92** (2008) 023104.

[28] H. W. Kihm, K. G. Lee, D. S. Kim, J. H. Kang and Q-H. Park. Control of surface plasmon generation efficiency by slit-width tuning. *Appl. Phys. Lett.* **92** (2008) 051115.

[29] T. Xu, Y. Zhao, D. Gan, C. Wang, C. Du and X. Luo. Directional excitation of surface plasmons with subwavelength slits. *Appl. Phys. Lett.* **92** (2008) 101501.

[30] L. Yin, V. K. Vlasko-Vlasov, A. Rydh, J. Pearson, U. Welp, S.-H. Chang, S. K. Gray, G. C. Schatz, D. B. Brown and C. W. Kimball. Surface plasmons at single nanoholes in Au films. *Appl. Phys. Lett.* **85** (2004) 467.

[31] J. Chandezon, M. T. Dupuis, G. Cornet and D. Mayster. Multicoated gratings: a differential formalism applicable in the entire optical region. *J. Opt. Soc. Am.* **72** (1982) 839.

[32] T. W. Priest, N. P. K. Cotter and J. R. Sambles. Periodic multilayer gratings of arbitrary shape. *J. Opt. Soc. Am. A* **12** (1995) 1740.

[33] N. P. K. Cotter, T. W. Priest and J. R. Sambles. Scattering matrix approach to multilayer diffraction. *J. Opt. Soc. Am. A* **12** (1995) 1097.

[34] J. P. Plumey, B. Guizal and J. Chandezon. Coordinate transformation method as applied to asymmetric gratings with vertical facets. *J. Opt. Soc. Am. A* **14** (1997) 610.

[35] L.Li. Multilayer-coated diffraction gratings: differential method of Chandezon *et al.* revisited. *J Opt. Soc. Am. A* **11** (1994) 2816.

[36] D. Maystre. Rigorous vector theories of diffraction gratings. In *Progress in*

Optics, ed. E Wolf (Amsterdam: Elsevier, 1984) **21**, 1.

[37] L. Li. Periodic multilayer gratings of arbitrary shape: Comment. *J. Opt. Soc. Am. A* **13** (1996) 1475

[38] N. P. K. Cotter, T. W. Priest and J. R. Sambles. Scattering-matrix approach to multilayer diffraction. *J. Opt. Soc. Am. A* **12** (1995) 1097.